Heterodi- and Heterotrinuclear Complexes Containing Highly Polar Metal−Metal Bonds†

Lutz H. Gade,*,‡ Stefan Friedrich,§ Dominique J. M. Trösch,§ Ian J. Scowen,|| and Mary McPartlin||

Laboratoire de Chimie Organométallique et de Catalyse, Institut LeBel, Université Louis Pasteur, 4 rue Blaise Pascal, 67070 Strasbourg, France, Institut für Anorganische Chemie der Universität Würzburg, Am Hubland, 97074 Würzburg, Germany, and School of Chemistry, University of North London, Holloway Road, London N7 8DB, U.K.

Received March 31, 1999

Reaction of the dichlorozirconium complex $[CH_2(CH_2NSiMe_3)_2ZrCl_2(thf)_2]$ (**1**), containing a chelating amido ligand and having a trans disposition of the chloro ligands established by an X-ray diffraction study, with the carbonylmetalate derivatives $K[MCp(CO)_2]$ ($Cp = C_5H_5$) and $Na[Co(CO)_3(PPh_3)]$ gave the heterotrinuclear complexes $[CH_2(CH_2NSiMe_3)_2Zr\{MCp(CO)_2\}_2]$ (M = Fe (**2**), Ru (**3**)) and $[CH_2(CH_2NSiMe_3)_2Zr\{Co(CO)_3(PPh_3)\}_2]$ (**4**), respectively. Of these, **2** and **3** were structurally characterized by X-ray crystallography, establishing two unsupported metal−metal bonds in each of the compounds [**2**, d(Zr−Fe) = 2.665(2), 2.664(2) Å; **3**, d(Zr−Ru) = 2.7372(7), 2.7452(7) Å]. Reaction of **2** and **3** with **1** in a 1:1 molar ratio led to a quantitative redistribution of complex fragments, yielding the dinuclear complexes $[CH_2(CH_2NSiMe_3)_2(Cl)Zr{-}MCp(CO)_2]$ (M = Fe (**5**), Ru (**6**). Both products as well as the Zr−Co complex $[CH_2(CH_2NSiMe_3)_2(Cl)Zr{-}Co(CO)_3(PPh_3)]$ (**7**) were also obtained in moderate yields by reacting **1** with 1 molar equiv of the carbonylmetalate. Reacting **5**−**7** with NaCp gave the corresponding CpZr complexes $[CH_2(CH_2NSiMe_3)_2(Cp)Zr{-}MCp(CO)_2]$ (M = Fe (**8**), Ru (**9**)) and $[CH_2(CH_2NSiMe_3)_2(Cp)Zr{-}Co(CO)_3(PPh_3)]$ (**10**), of which **9** was characterized by a single-crystal X-ray structure analysis [d(Zr−Ru) = 2.8297(14) Å]. Compounds **5**, **6**, **8**, and **9** insert methyl isonitrile to give the heterobimetallic metallaiminoacylzirconium complexes $[CH_2(CH_2NSiMe_3)_2(Cl)Zr\{\eta^2\text{-}C(=NCH_3)MCp(CO)_2\}]$ (M = Fe (**11**), Ru (**12**)) and $[CH_2(CH_2NSiMe_3)_2(Cp)Zr\{\eta^2\text{-}C(=NCH_3)MCp(CO)_2\}]$ (M = Fe (**13**), Ru (**14**)), respectively. Reaction of the heterotrinuclear compounds **2** and **3** with isonitriles exclusively gave the products of the insertion into one of the unsupported metal−metal bonds, $[CH_2(CH_2NSiMe_3)_2Zr\{\eta^2\text{-}C(=NCH_3)MCp(CO)_2\}\{MCp(CO)_2\}]$ (M = Fe, R = Me, ^{n}Bu, Cy, Tol (**15a**−**d**); M = Ru, R = Me, ^{n}Bu, Cy, Tol (**16a**−**d**)). A crystal structure analysis of **16a** established the insertion into one of the metal−metal bonds while the intact Zr−Ru bond was elongated in comparison to that of **3** [d(Zr−Ru) = 2.8639(6) Å]. Cleavage of both metal−metal bonds in **2** and **3** was observed in reactions with sulfoxides. Transfer of the S-bound oxygen atom to a carbonyl ligand led to CO_2-linked trinuclear complexes in which the thioether thus generated was coordinated to the late transition metal center. The reaction at the two metal−metal bonds occurred cooperatively, precluding the isolation of intermediates.

Introduction

The recent development of polydentate amido complex chemistry has not only considerably extended the use of early transition metal complexes in stoichiometric[1−7] and catalytic[8−11] conversions of organic substrates but has also offered new opportunities for their use as building blocks in oligonuclear metal−metal bonded systems which hitherto were considered to be intrinsically labile.[12−18] In particular, the use of tripodal amido ligands in the synthesis of directly metal−metal bonded M−M′ heterobimetallic compounds (M = Ti, Zr, Hf; M′ = late transition metal) resulted in systems of unprecedented stability.[19−21] Apart from the kinetic stabilization due to steric

† Dedicated to Professor Raymond Weiss on the occasion of his 70th birthday.

‡ Université Louis Pasteur. E-mail: gade@chimie.u-strasbg.fr.
§ Universität Würzburg.
|| University of North London.

(1) Schrock, R. R. *Acc. Chem. Res.* **1997**, *30*, 9.
(2) Guerin, F.; McConville, D. H.; Vittal, J. J. *Organometallics* **1995**, *14*, 3154.
(3) Cloke, F. G. N.; Hitchcock, P. B.; Love, J. B. *J. Chem. Soc., Dalton Trans.* **1995**, 25.
(4) Memmler, H.; Walsh, K.; Gade, L. H.; Lauher, J. W. *Inorg. Chem.* **1995**, *34*, 4062.
(5) Freundlich, J. S.; Schrock, R. R.; Davis, W. M. *J. Am. Chem. Soc.* **1996**, *118*, 3643.
(6) Mösch-Zanetti, N. C.; Schrock, R. R.; Davis, W. M.; Wanninger, K.; Seidel, S. W.; O'Donoghue, M. B. *J. Am. Chem. Soc.* **1997**, *119*, 11037.
(7) Schrock, R. R.; Seidel, S. W.; Mösch-Zanetti, N. C.; Shih, K.-Y.; O'Donoghue, M. B.; Davis, W. M.; Reiff, W. M. *J. Am. Chem. Soc.* **1997**, *119*, 11876.
(8) Scollard, J. D.; McConville, D. H. *J. Am. Chem. Soc.* **1996**, *118*, 10008.
(9) Scollard, J. D.; McConville, D. H.; Vittal, J. J. *Organometallics* **1995**, *14*, 5478.
(10) Baumann, R.; Davis, W. M.; Schrock, R. R. *J. Am. Chem. Soc.* **1997**, *119*, 3830.
(11) Horton, A. D.; de Woth, J. *Chem. Commun.* **1996**, 1375.
(12) Stephan, D. W. *Coord. Chem. Rev.* **1989**, *95*, 41.
(13) Casey, C. P. *J. Organomet. Chem.* **1990**, *400*, 205.
(14) Herberhold, M.; Jin, G.-X. *Angew. Chem., Int. Ed. Engl.* **1994**, *33*, 964.
(15) Sartain, W. S.; Selegue, J. P. *J. Am. Chem. Soc.* **1985**, *107*, 5818.
(16) Sartain, W. S.; Selegue, J. P. *Organometallics* **1987**, *6*, 1812.
(17) Sartain, W. S.; Selegue, J. P. *Organometallics* **1989**, *8*, 2153.
(18) Selent, D.; Beckhaus, R.; Pickardt, J. *Organometallics* **1993**, *12*, 2857.
(19) Friedrich, S.; Memmler, H.; Gade, L. H.; Li, W.-S.; McPartlin, M. *Angew. Chem., Int. Ed. Engl.* **1994**, *33*, 676.
(20) Findeis, B.; Schubart, M.; Platzek, C.; Gade, L. H.; Scowen, I. J.; McPartlin, M. *Chem. Commun.* **1996**, 219.
(21) Friedrich, S.; Memmler, H.; Gade, L. H.; Li, W.-S.; Scowen, I. J.; McPartlin, M.; Housecroft, C. E. *Inorg. Chem.* **1996**, *35*, 2433.

10.1021/ic990350q CCC: $18.00
Published on Web 10/23/1999

Chart 1

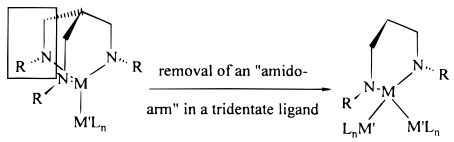

shielding of the metal−metal bond by the ligand periphery, the coordination of the amido tripod to a high-valent metal generates a fairly rigid cage structure in which the geometry of the early transition metal complex fragment is fixed in such a way that geometric "relaxation" upon cleavage of the metal−metal bond is suppressed. This situation is responsible for an additional thermodynamic stabilization of the dinuclear compounds.[22,23] The coordination of the trianionic tripodal amido ligands to tetravalent group 4 metals leads to *monofunctional* building blocks containing a single displaceable anion ligand which, upon salt metathesis with an anionic metal complex, may form a single metal−metal bond in heteronuclear complexes. In an extension of this strategy, *difunctional* amido complex units which contain two displaceable anionic ligands therefore may be employed in the synthesis of trinuclear or oligonuclear heterobimetallic complexes. This requires the use of dianionic ligand systems for the early transition metal complex fragment. (See Chart 1.)

Heterotrinuclear complexes possessing two highly polar metal−metal bonds are particularly rare, the only fully characterized and studied example being Casey's $ZrRu_2$ complex $[Cp_2Zr\{Ru(CO)_2Cp\}_2]$ ($Cp = C_5H_5$).[24] More recently, Pályi et al. gave a preliminary account of the generation of $[Cp_2Zr\{Co(CO)_4\}_2]$ by salt metathesis or alkane elimination.[25] We recently developed several new amido ligands to be employed in difunctional building blocks for heterooligonuclear complexes, among them tripodal diamido−pyridine systems.[26−28] However, for the synthesis of heterotrinuclear complexes derived from a difunctional group 4 complex fragment, the use of a simple bidentate chelating amido ligand proved to be most successful. On the basis of early work by Bürger et al.,[29−32] we synthesized the difunctional amidozirconium complexes of the type $[CH_2(CH_2NSiMe_3)_3ZrCl_2(D)_2]$ (D = thf, pyridine), which proved to be ideally suited for the preparation of such trinuclear complexes.[33] Additionally, their relative thermal stability has opened the possibilty to study their reactivity toward organic substrates and to investigate the possible cooperative reactive behavior of the different complex fragments bonded to each other.[34−40]

In this paper, we report the synthesis and structural characterization of several new heterodi- and heterotrinuclear complexes based on the $\{CH_2(CH_2NSiMe_3)_2Zr\}$ fragment, as well as some fundamental aspects of their reactivity.

Experimental Section

All manipulations were performed under an inert gas atmosphere of dried argon in standard (Schlenk) glassware which was flame-dried with a Bunsen burner prior to use. Solvents were dried according to standard procedures and saturated with Ar. The deuterated solvents used for the NMR spectroscopic measurements were degassed by three successive "freeze−pump−thaw" cycles and dried over 4 Å molecular sieves.

The ^1H, ^{13}C, ^{29}Si, and ^{31}P NMR spectra were recorded on a Bruker AC 200 spectrometer equipped with a B-VT-2000 variable-temperature unit (at 200.13, 50.32, 39.76, and 81.03 MHz, respectively) with tetramethylsilane and H_3PO_4 (85%, external) as references. Infrared spectra were recorded on Perkin-Elmer 1420 and Bruker IRS 25 FT spectrometers.

Elemental analyses were carried out in the microanalytical laboratory of the chemistry department of the University of Würzburg. The complex $[CH_2(CH_2NSiMe_3)_2ZrCl_2(thf)_2]$ (**1**) was prepared as reported previously by us.[41] The salts of the transition metal carbonylates $K[CpFe(CO)_2]$, $K[CpRu(CO)_2]$, and $Na[Co(CO)_3(PPh_3)]$ were synthesized by literature methods.[42,43] All other chemicals used as starting materials were obtained commercially and used without further purification.

(1) Preparation of $[CH_2(CH_2NSiMe_3)_2Zr\{Fe(CO)_2Cp\}_2]$ (2). To a mixture of solid $[CH_2(CH_2NSiMe_3)_2ZrCl_2(thf)_2]$ (**1**) (550 mg = 1.05 mmol) and 460 mg (2.12 mmol) of $K[CpFe(CO)_2]$ were added 20 mL of toluene and 2 mL of THF at ambient temperature. After 1 h of stirring, 20 mg of Na powder was added to the reaction mixture. Stirring was continued for another 1 h, the solvent was then removed in vacuo, and the residue was extracted with 25 mL of pentane. After filtration, the solvent of the filtrate was again removed in vacuo and the residue was recrystallized from 4 mL of diethyl ether at −78 °C. Compound **2** was obtained as a yellow crystalline solid. Yield: 260 mg (37%). Mp: 88 °C. IR (toluene): 2900 m, 2850 m, 2005 s, 1941 vs, 1888 vs, 1245 m, 1030 w, 920 w, 889 w, 855 s, 835 s, 795 w cm^{-1}. ^1H NMR (C_6D_6): δ 0.43 [s, $Si(CH_3)_3$], 1.31 (m, CH_2), 3.32 (m, CH_2N), 4.56 (s, C_5H_5). ^{13}C NMR (C_6D_6): δ 1.6 [$Si(CH_3)_3$], 33.0 (CH_2), 43.4 (CH_2N), 82.8 (C_5H_5), 216.3 (*C*O). ^{29}Si NMR (C_6D_6): δ 2.2. Anal. Calcd for $C_{23}H_{34}Fe_2N_2O_4Si_2Zr$: C, 41.75; H, 5.18; N, 4.23. Found: C, 41.83; H, 5.32; N, 4.12.

(2) Preparation of $[CH_2(CH_2NSiMe_3)_2Zr\{Ru(CO)_2Cp\}_2]$ (3). To a mixture of solid $[CH_2(CH_2NSiMe_3)_2ZrCl_2(thf)_2]$ (**1**) (980 mg = 1.87 mmol) and 1.00 g (3.83 mmol) of $K[CpRu(CO)_2]$ were added 30 mL of toluene and 2 mL of THF at ambient temperature. After 12 h of stirring, the volume of the solution was reduced to ca. 20 mL. After filtration, the solvent of the filtrate was removed in vacuo and the residue was recrystallized from 5 mL of diethyl ether at −78 °C. Compound **3** was obtained as an orange crystalline solid. Yield: 1.03 g (73%). Mp: 92 °C. IR (toluene): 2858 s, 2016 m, 1968 vs, 1908 vs, 1365 vw, 1250 m, 1070 vs, 912 s, 842 s, 802 m cm^{-1}. ^1H NMR

(22) Jansen, G.; Schubart, M.; Findeis, B.; Gade, L. H.; Scowen, I. J.; McPartlin, M. *J. Am. Chem. Soc.* **1998**, *120*, 7239.
(23) Schubart, M.; Mitchell, G.; Gade, L. H.; Scowen, I. J.; McPartlin, M. *Chem. Commun.* **1999**, 233.
(24) Casey, C. P.; Jordan, R. F.; Rheingold, A. L. *Organometallics* **1984**, *3*, 504.
(25) Bartik, T.; Windisch, H.; Sorkau, A.; Thiele, K.-H.; Kriebel, C.; Herfurth, A.; Tschoerner, M.; Zucchi, G.; Pályi, G. *Inorg. Chim. Acta* **1994**, *227*, 201.
(26) Friedrich, S.; Gade, L. H.; Edwards, A. J.; McPartlin, M. *J. Chem. Soc., Dalton Trans.* **1993**, 2861.
(27) Friedrich, S.; Schubart, M.; Gade, L. H.; Scowen, I. J.; Edwards, A. J.; McPartlin, M. *Chem. Ber.* **1997**, *130*, 1751.
(28) Blake, A. J.; Collier, P. E.; Gade, L. H.; McPartlin, M.; Mountford, P.; Schubart, M.; Scowen, I. J. *Chem. Commun.* **1997**, 1555.
(29) Bürger, H.; Beiersdorf, D. *Z. Anorg. Allg. Chem.* **1979**, *459*, 111.
(30) Wiegel, K.; Bürger, H. *Z. Anorg. Allg. Chem.*. **1976**, *426*, 301.
(31) Brauer, D. J.; Bürger, H.; Essig, E.; Gschwandtner, W. *J. Organomet. Chem.* **1980**, *190*, 343.
(32) Bürger, H.; Gschwandtner, W.; Liewald, G. R. *J. Organomet. Chem.* **1983**, *259*, 145.
(33) Friedrich, S.; Gade, L. H.; Scowen, I. J.; McPartlin, M. *Angew. Chem., Int. Ed. Engl.* **1996**, *35*, 1338.
(34) Casey, C. P.; Palermo, R. E.; Jordan, R. F. *J. Am. Chem. Soc.* **1985**, *107*, 4597.
(35) Casey, C. P.; Palermo, R. E. *J. Am. Chem. Soc.* **1986**, *108*, 549.
(36) Ozawa, F.; Park, J. W.; Mackenzie, P. B.; Schaefer, W. P.; Henling, L. M.; Grubbs, R. H. *J. Am. Chem. Soc.* **1989**, *111*, 1319.
(37) Baranger, A. M.; Bergman, R. G. *J. Am. Chem. Soc.* **1994**, *116*, 3822.
(38) Hanna, T. A.; Baranger, A. M.; Bergman, R. G. *J. Am. Chem. Soc.* **1995**, *117*, 665.
(39) Baranger, A. M.; Hanna, T. A.; Bergman, R. G. *J. Am. Chem. Soc.* **1995**, *177*, 10041.
(40) Hanna, T. A.; Baranger, A. M.; Bergman, R. G. *J. Am. Chem. Soc.* **1995**, *117*, 11363.
(41) Friedrich, S.; Gade, L. H.; Scowen, I. J.; McPartlin, M. *Organometallics* **1995**, *14*, 5344.
(42) Brookhart, M.; Studabaker, W. B.; Husk, R. *Organometallics* **1987**, *6*, 1141.
(43) Seyferth, D.; Millar, M. D. *J. Organomet. Chem.* **1972**, *38*, 373.

(C_6D_6): δ 0.48 [s, Si(CH_3)$_3$], 1.34 (m, CH_2), 3.17 (m, CH_2N), 4.91 (s, C_5H_5). ^{13}C NMR (C_6D_6): δ 1.8 [Si(CH_3)$_3$], 35.5 (CH_2), 45.6 (CH_2N), 85.7 (C_5H_5), 205.1 (CO). ^{29}Si NMR (C_6D_6): δ 1.7. Anal. Calcd for $C_{23}H_{34}N_2O_4Ru_2Si_2Zr$: C, 36.73; H, 4.56; N, 3.73. Found: C, 36.65; H, 4.48; N, 3.75.

(3) Preparation of [CH$_2$(CH$_2$NSiMe$_3$)$_2$Zr{Co(CO)$_3$(PPh$_3$)}$_2$] (4). To a mixture of solid [CH$_2$(CH$_2$NSiMe$_3$)$_2$ZrCl$_2$(thf)$_2$] (**1**) (1.02 g = 1.95 mmol) and 1.27 g (2.22 mmol) of Na[Co(CO)$_3$(PPh$_3$)](thf)$_2$, which was cooled to −45 °C, was slowly added 20 mL of cold toluene. The reaction mixture was slowly warmed to room temperature and stirred for another 30 min. After removal of the solvent in vacuo, the residue was extracted with 50 mL of pentane, the extract was filtered, and the volume of the extract was reduced to ca. 10 mL. Storage at −78 °C yielded **4** as a yellow solid. Yield: 679 mg (31%). IR (toluene): 2850 w, 2042 vw, 1962 s, 1925 vs, 1915 vs, 1445 m, 1250 m, 1188 vw, 1094 m, 1070 m, 1039 w, 1001 vw, 910 m, 842 s, 808 m cm^{-1}. ^{1}H NMR (C_6D_6): δ 0.37 [s, Si(CH_3)$_3$], 1.22 (m, CH_2), 3.39 (m, CH_2N), 6.93−7.02, 7.52−7.69 [m, P(C_6H_5)$_3$]. ^{13}C NMR (C_6D_6): δ 0.9 [Si(CH_3)$_3$], 30.2 (CH_2), 43.3 (CH_2N), 128.9 [d, ^3J(PC) = 10.2 Hz, C^{3,5} of C_6H_5], 130.0 (s, C^4 of C_6H_5), 133.5 [d, ^2J(PC) = 11.6 Hz, C^{2,6} of C_6H_5], 135.7 [d, ^1J(PC) = 41.4 Hz, C^1 of C_6H_5], 206.6 [br, CO, ^2J(PC) not resolved]. ^{29}Si NMR (C_6D_6): δ 4.0. ^{31}P NMR (C_6D_6): δ 60.0 (s, br). Anal. Calcd for $C_{51}H_{54}Co_2N_2O_6P_2Si_2Zr$: C, 54.78; H, 4.87; N, 2.51. Found: C, 54.02; H, 4.61; N, 2.36.

(4) Preparation of [CH$_2$(CH$_2$NSiMe$_3$)$_2$(Cl)Zr−Fe(CO)$_2$Cp] (5). (a) From [CH$_2$(CH$_2$NSiMe$_3$)$_2$ZrCl$_2$(thf)$_2$] (1) and K[CpFe(CO)$_2$]. To a mixture of solid [CH$_2$(CH$_2$NSiMe$_3$)$_2$ZrCl$_2$(thf)$_2$] (**1**) (1.73 g = 3.31 mmol) and 715 mg (3.31 mmol) K[CpFe(CO)$_2$], which was cooled to −60 °C, was slowly added 100 mL of cold toluene. The reaction mixture was warmed to room temperature over a period of 16 h. After filtration, the solvent was removed in vacuo and the residue was recrystallized from 5 mL of diethyl ether at −78 °C. Compound **5** was obtained as a yellow crystalline solid. Yield: 235 mg (14%).

(b) from [CH$_2$(CH$_2$NSiMe$_3$)$_2$ZrCl$_2$(thf)$_2$] (1) and [CH$_2$(CH$_2$NSiMe$_3$)$_2$Zr{Fe(CO)$_2$Cp}$_2$] (2). Solid **1** (260 mg = 0.5 mmol) and **2** (330 mg = 0.5 mmol) were dissolved in 10 mL of C_6H_6, and the mixture was stirred for 24 h, after which the conversion to **5** was complete. The solid product was isolated in almost quantitative yield after removal of the solvent in vacuo and washing of the residue with cold pentane.

IR (toluene): 2970 w, 2870 vw, 2840 vw, 2007 w, 1947 vs, 1895 vs, 1246 m, 1088 vw, 1064 m. 887 m, 840 s, 803 m, 743 w cm^{-1}. ^{1}H NMR (C_6D_6): δ 0.37 [s, Si(CH_3)$_3$], 1.40 [dtt, ^2J(H^{c}H^d) = 14.2 Hz, ^3J(H^{a}H^d) = ^3J(H$^{a'}$H^d) = 8.8 Hz, ^3J(H^{b}H^d) = ^3J(H$^{b'}$H^c) = 2.9 Hz, H^d of CHH], 2.05 [dtt, ^3J(H^{a}H^c) = ^3J(H^{a}H^c) = 2.5 Hz, ^3J(H^{b}H^c) = ^3J(H$^{b'}$H^c) = 7.0 Hz, H^c of CHH], 3.23 [ddd, ^2J(H^{a}H^b) = ^2J(H$^{a'}$H$^{b'}$) = 13.7 Hz, H$^{b/b'}$ of CHHN], 3.44 [ddd, H$^{a/a'}$ of CHHN], 4.47 (s, C_5H_5). ^{13}C NMR (C_6D_6): δ 0.4 [Si(CH_3)$_3$], 38.4 (CH_2), 51.8 (CH_2N), 81.8 (C_5H_5), 215.7 (CO). ^{29}Si NMR (C_6D_6): δ 1.3. Anal. Calcd for $C_{16}H_{29}ClFeN_2O_2Si_2Zr$: C, 36.95; H, 5.62; N, 5.39. Found: C, 37.11; H, 5.51; N, 5.45.

(5) Preparation of [CH$_2$(CH$_2$NSiMe$_3$)$_2$(Cl)Zr−Ru(CO)$_2$Cp] (6). (a) From [CH$_2$(CH$_2$NSiMe$_3$)$_2$ZrCl$_2$(thf)$_2$] (1) and K[CpRu(CO)$_2$]. To a mixture of solid [CH$_2$(CH$_2$NSiMe$_3$)$_2$ZrCl$_2$(thf)$_2$] (**1**) (2.00 g = 3.84 mmol) and 1.00 g (3.84 mmol) of K[CpRu(CO)$_2$], which was cooled to −60 °C, were slowly added 50 mL of cold toluene and 5 mL of cold THF. The reaction mixture was warmed to room temperature over a period of 16 h. After removal of the solvent in vacuo, the residue was extracted with 100 mL of pentane, the extract was filtered, the solvent was removed, and the solid orange residue was dried under high vacuum. Yield: 1.69 g (78%).

(b) from [CH$_2$(CH$_2$NSiMe$_3$)$_2$ZrCl$_2$(thf)$_2$] (1) and [CH$_2$(CH$_2$NSiMe$_3$)$_2$Zr{Ru(CO)$_2$Cp}$_2$] (3). Solid **1** (260 mg = 0.5 mmol) and **3** (375 mg = 0.5 mmol) were dissolved in 10 mL of C_6H_6, and the mixture was stirred for 24 h, after which the conversion to **6** was complete. The solid product was isolated in almost quantitative yield after removal of the solvent in vacuo and washing of the residue with cold pentane.

IR (toluene): 2890 w, 2830 w, 2017 m, 1968 vs, 1908 vs, 1298 s, 1088 w, 1060 w, 885 m, 842 vs, 802 s, 745 w cm^{-1}. ^{1}H NMR (C_6D_6): δ 0.39 [s, Si(CH_3)$_3$], 1.52 [dtt, ^2J(H^{c}H^d) = 15.0 Hz, ^3J(H^{a}H^d) = ^3J(H$^{a'}$H^d) = 8.0 Hz, ^3J(H^{b}H^d) = ^3J(H$^{b'}$H^d) = 2.8 Hz, H^d of CHH], 2.07 [dtt, ^3J(H^{a}H^c) = ^3J(H$^{a'}$H^c) = 2.7 Hz, ^3J(H^{b}H^c) = ^3J(H$^{b'}$H^c) = 7.7 Hz, H^c of CHH], 3.21 [ddd, ^2J(H^{a}H^b) = ^2J(H$^{a'}$H$^{b'}$) = 13.0 Hz, H$^{b/b'}$ of CHHN], 3.40 (ddd, H$^{a/a'}$ of CHHN), 4.94 (s, C_5H_5). ^{13}C NMR (C_6D_6): δ 0.4 [Si(CH_3)$_3$], 38.5 (CH_2), 52.1 (CH_2N), 84.8 (C_5H_5), 204.9 (CO). ^{29}Si NMR (C_6D_6): δ 1.1. Anal. Calcd for $C_{16}H_{29}ClN_2O_2RuSi_2Zr$: C, 33.99; H, 5.17; N, 4.96. Found: C, 34.11; H, 5.31; N, 4.85.

(6) Preparation of [CH$_2$(CH$_2$NSiMe$_3$)$_2$(Cl)Zr−Co(CO)$_3$(PPh$_3$)] (7). To a mixture of solid [CH$_2$(CH$_2$NSiMe$_3$)$_2$ZrCl$_2$(thf)$_2$] (**1**) (504 g = 0.96 mmol) and 554 mg (0.97 mmol) of Na[Co(CO)$_3$(PPh$_3$)](thf)$_2$, which was cooled to −60 °C, was slowly added 20 mL of cold toluene. The reaction mixture was slowly warmed to 0 °C and stirred for another 20 min. After removal of the solvent in vacuo, the residue was extracted with 50 mL of pentane, the extract was filtered, and the volume of the solution was reduced to ca. 5 mL. Storage at −78 °C yielded **7** as a yellow solid. Yield: 330 mg (46%). IR (toluene): 2870 w, 2860 m, 2040 w, 1963 vs, 1592 s, 1372 m, 1245 m, 1175 m, 1070 m, 1045 m, 1025 m, 892 m, 838 s cm^{-1}. ^{1}H NMR (C_6D_6): δ 0.44 [s, Si(CH_3)$_3$], 1.43 (m, H^d of CHH), 2.14 (m, H, H^c of CHH), 3.28 [ddd, ^2J(H^{a}H^b) = ^2J(H$^{a'}$H$^{b'}$) = 13.7 Hz, ^3J(H^{b}H^c) = ^3J(H$^{b'}$H^c) = 6.4 Hz, ^3J(H^{b}H^d) = ^3J(H$^{b'}$H^d) = 3.0 Hz, H$^{b/b'}$ of CHHN], 3.49 [ddd, ^3J(H^{a}H^d) = ^3J(H$^{a'}$H^d) = 9.1 Hz, ^3J(H^{a}H^c) = ^3J(H$^{a'}$H^c) = 2.4 Hz, H$^{a/a'}$ of CHHN], 6.96−7.02, 7.52−7.69 [m, P(C_6H_5)$_3$]. ^{13}C NMR (C_6D_6): δ 0.1 [Si(CH_3)$_3$], 38.2 (CH_2), 51.5 (CH_2N), 129.1 [d, ^3J(PC) = 10.3 Hz, C^{3,5} of C_6H_5], 130.1 (s, C^4 of C_6H_5), 133.4 [d, ^2J(PC) = 11.9 Hz, C^{2,6} of C_6H_5], 135.7 [d, ^1J(PC) = 40.9 Hz, C^1 of C_6H_5], 206.5 [br, CO, ^2J(PC) not resolved]. ^{29}Si NMR (C_6D_6): δ 2.7. ^{31}P NMR (C_6D_6): δ 60.1 (s, br). Anal. Calcd for $C_{30}H_{39}ClCoN_2O_3PSi_2Zr$: C, 48.15; H, 5.25; N, 3.74. Found: C, 48.28; H, 5.48; N, 3.63.

(7) Preparation of [CH$_2$(CH$_2$NSiMe$_3$)$_2$(Cp)Zr−Fe(CO)$_2$Cp)] (8), [CH$_2$(CH$_2$NSiMe$_3$)$_2$(Cp)Zr−Fe(CO)$_2$Cp] (9), and [CH$_2$(CH$_2$NSiMe$_3$)$_2$-(Cp)Zr−Co(CO)$_3$PPh3] (10) from 5−7. Solid [CH$_2$(CH$_2$NSiMe$_3$)$_2$-(Cl)Zr−M(CO)$_2$Cp] (M = Fe (**5**), Ru (**6**)) or [CH$_2$(CH$_2$NSiMe$_3$)$_2$(Cl)Zr−Co(CO)$_3$PPh$_3$] (**7**) (1.0 mmol) was placed in a Schlenk tube together with 88 mg (1 mmol) of solid NaCp. To this was added 5 mL of toluene which was precooled to −70 °C, and the reaction mixture was warmed to ambient temperature over a period of 15 h. After centrifugation, the solution obtained was evaporated to dryness and the yellow solid residue was washed with 2 mL of cold pentane to yield the previously characterized compounds **8**−**10** in almost quantitative yields.[13]

(8) Preparation of [CH$_2$(CH$_2$NSiMe$_3$)$_2$(Cl)Zr{η^2-C(=NCH$_3$)-M(CO)$_2$Cp}] (M = Fe (11), Ru (12)). To a solution of 1.0 mmol of [CH$_2$(CH$_2$NSiMe$_3$)$_2$(Cl)Zr−M(CO)$_2$Cp] (M = Fe (**5**), Ru (**6**)) in 5 mL of C_6H_6 was added 57 μL of CH$_3$NC (1.0 mmol). The ^{1}H NMR spectra indicated the quantitative formation of **11** and **12**, respectively. Both compounds were not isolated due to partial thermal decomposition upon removal of the solvent in vacuo.

(a) 11. IR (toluene): 2895 vw, 2830 vw, 2020 vs, 1965 vs, 1556 w, 1420 vw, 1250 m, 1065 vw, 1045 vw, 960 w, 895 m, 842 s, 752 w cm^{-1}. ^{1}H NMR (C_6D_6): δ 0.01 [s, Si(CH_3)$_3$], 1.90 (m, H^d of CHH), 2.40 (m, H^c of CHH), 3.37 [ddd, ^2J(H^{a}H^b) = ^2J(H$^{a'}$H$^{b'}$) = 12.9 Hz, ^3J(H^{b}H^c) = ^3J(H$^{b'}$H^c) = 8.0 Hz, ^3J(H^{b}H^d) = ^3J(H$^{b'}$H^d) = 2.6 Hz, H$^{b/b'}$ of CHHN], 3.49 [ddd, ^3J(H^{a}H^d) = ^3J(H$^{a'}$H^d) = 7.5 Hz, ^3J(H^{a}H^c) = ^3J(H^{a}H^c) = 2.8 Hz, H$^{a/a'}$ of CHHN], 3.66 (s, NCH_3), 4.65 (s, C_5H_5). ^{13}C NMR (C_6D_6): δ −0.3 [Si(CH_3)$_3$], 40.1 (CH_2), 44.7 (NCH_3), 51.1 (CH_2N), 89.6 (C_5H_5), 214.8 (CO), 286.2 (C=N). ^{29}Si NMR (C_6D_6): δ −2.2.

(b) 12. IR (benzene): 2980 m, 2945 w, 2920 w, 2026 vs, 1980 vs, 1565 w, 1445 w, 1372 m, 1270 m, 1258 s, 1092 m, 1072 m, 1018 w, 978 w, 948 w, 900 s, 850 vs, 812 s, 752 m cm^{-1}. ^{1}H NMR (C_6D_6): δ 0.01 [s, Si(CH_3)$_3$], 1.90 (m, H^d of CHH), 2.46 (m, H^c of CHH), 3.37 [ddd, ^2J(H^{a}H^b) = ^2J(H$^{a'}$H$^{b'}$) = 12.9 Hz, ^3J(H^{b}H^c) = ^3J(H$^{b'}$H^c) = 8.3 Hz, ^3J(H^{b}H^d) = ^3J(H$^{b'}$H^d) = 2.6 Hz, H$^{b/b'}$ of CHHN], 3.50 [ddd, ^3J(H^{a}H^d) = ^3J(H$^{a'}$H^d) = 7.4 Hz, ^3J(H^{a}H^c) = ^3J(H$^{a'}$H^c) = 2.8 Hz, H$^{a/a'}$ of CHHN], 3.60 (s, NCH_3), 5.11 (s, C_5H_5). ^{13}C NMR (C_6D_6): δ −0.2 [Si(CH_3)$_3$], 39.8 (CH_2), 46.3 (NCH_3), 50.9 (CH_2N), 92.5 (C_5H_5), 199.9 (CO), 276.2 (C=N). ^{29}Si NMR (C_6D_6): δ −2.3.

(9) Preparation of [CH$_2$(CH$_2$NSiMe$_3$)$_2$(Cp)Zr{η^2-C(=NCH$_3$)-M(CO)$_2$Cp}] (M = Fe (13), Ru (14)). To a solution of 0.28 mmol of [CH$_2$(CH$_2$NSiMe$_3$)$_2$(Cp)Zr−M(CO)$_2$Cp] (M = Fe (**13**), Ru (**14**)) in 5 mL of toluene was added 16 μL of CH$_3$NC (0.28 mmol). After 5 min of stirring at room temperature, the solvent was removed in vacuo and the solid residue was extracted with 5 mL of diethyl ether. Upon

filtration, the solution was concentrated to ca. 3 mL and stored at −60 °C. Compounds **13** and **14** were obtained as yellow crystalline solids.

(a) 13. Yield: 114 mg (69%). IR (toluene): 2880 vw, 2840 vw, 1997 vs, 1942 vs, 1548m, 1390 w, 1348 w, 1245 s, 1120 w, 1050 w, 1012 m, 952 m, 935 m, 860 s, 832 vs, 794 s cm^{-1}. ^{1}H NMR (C_6D_6): δ 0.08 [s, Si(CH_3)$_3$], 1.10 (m, CHH), 1.51 (m, CHH), 3.03 (m, CH_2N), 3.53 (s, NCH_3), 4.58 [s, (C_5H_5)Fe], 6.16 [s, (C_5H_5)Zr]. ^{13}C NMR (C_6D_6): δ 1.8 [Si(CH_3)$_3$], 35.2 (CH_2), 45.8 (CH_2N), 46.7 (NCH_3), 89.0 [(C_5H$_5$)Fe], 109.2 [(C_5H$_5$)Zr], 215.8 (CO), 286.2 (C═N). ^{29}Si NMR (C_6D_6): δ −2.8. Anal. Calcd for $C_{23}H_{37}FeN_3O_2Si_2Zr$: C, 46.76; H, 6.31; N, 7.11. Found: C, 46.58; H, 6.49; N, 7.28.

(b) 14. Yield: 60 mg (78%). IR (toluene): 2880 vw, 2840 vw, 2015 vs, 1955 vs, 1395 w, 1232 s, 1182 vs, 1135 w, 1115 w, 1049 vw, 1015 vw, 935 vw, 860 w, 835 m, 815 m, 795 w cm^{-1}. ^{1}H NMR (C_6D_6): δ 0.09 [s, Si(CH_3)$_3$], 1.10 (m, CHH), 1.56 (m, CHH), 3.03 (m, CH_2N), 3.47 (s, NCH_3), 5.09 [s, (C_5H_5)Ru], 6.16 [s, (C_5H_5)Zr]. ^{13}C NMR (C_6D_6): δ 1.8 [Si(CH_3)$_3$], 35.6 (CH_2), 46.1 (CH_2N), 48.1 (NCH_3), 92.3 [(C_5H$_5$)Ru], 109.1 [(C_5H$_5$)Zr], 200.8 (CO), 275.6 (C═N). ^{29}Si NMR (C_6D_6): δ −3.0. Anal. Calcd for $C_{23}H_{37}N_3O_2RuSi_2Zr$: C, 43.43; H, 5.86; N, 6.61. Found: C, 43.28; H, 5.69; N, 6.68.

(10) General Preparative Procedure for [CH$_2$(CH$_2$NSiMe$_3$)$_2$Zr{η^2-C(═NR)M(CO)$_2$Cp}{M(CO)$_2$Cp}] (M = Fe, R = Me, ^{n}Bu, Cy, *p*-Tol (15a−d); M = Ru (16a−d)). To a solution of 0.29 mmol of [CH$_2$(CH$_2$NSiMe$_3$)$_2$Zr{M(CO)$_2$Cp}$_2$] (M = Fe (**2**), Ru (**3**)) in 5 mL of toluene was added 0.29 mmol of RNC (using a microliter syringe). After 5 min of stirring at room temperature, the solvent was removed in vacuo, and the solid residue was extracted with 5 mL of diethyl ether. Upon filtration, the solution was concentrated to ca. 3 mL and stored at −60 °C. Compounds **15a**−**d** and **16a**−**d** were obtained as orange-red and yellow crystalline solids, respectively.

(a) 15a. Yield: 126 mg (62%). IR (benzene): 2955 vw, 2895 vw, 2850 vw, 2005 vs, 1951 vs, 1924 vs, 1862 vs, 1542 w, 1415 vw, 1378 vw, 1323 vw, 1245 m, 1112 vw, 1090 vw, 1042 w, 1025 vw, 953 w, 892 m, 840 vs, 809 s, 748 w cm^{-1}. ^{1}H NMR (C_6D_6): δ 0.07 [s, Si(CH_3)$_3$], 1.43 (m, H^d of CHH), 2.31 (m, H^c of CHH), 3.38 [ddd, ^2J(H^{a}H^b) = ^2J(H$^{a'}$H$^{b'}$) = 14.2 Hz, ^3J(H^{b}H^c) = ^3J(H$^{b'}$H^c) = 5.1 Hz, ^3J(H^{b}H^d) = ^3J(H$^{b'}$H^d) = 3.0 Hz, H$^{b/b'}$ of CHHN], 3.64 [ddd, ^3J(H^{a}H^d) = ^3J(H$^{a'}$H^d) = 10.8 Hz, ^3J(H^{a}H^c) = ^3J(H$^{a'}$H^c) = 1.9 Hz, H$^{a/a'}$ of CHHN], 3.95 (s, NCH_3), 4.50 [s, (C_5H_5)Fe−Zr], 4.54 [s, (C_5H_5)Fe−C]. ^{13}C NMR (C_6D_6): δ 0.5 [Si(CH_3)$_3$], 41.2 (CH_2), 47.0 (NCH_3), 50.4 (CH_2N), 80.9 [(C_5H$_5$)Fe−Zr], 90.2 [(C_5H$_5$)Fe−C], 215.0 [(CO)$_2$Fe−C], 220.1 [(CO)$_2$Fe−Zr], 283.2 (C═N). ^{29}Si NMR (C_6D_6): δ −1.1. Anal. Calcd for $C_{25}H_{37}Fe_2N_3O_4Si_2Zr$: C, 42.73; H, 5.31; N, 5.98. Found: C, 43.09; H, 5.69; N, 5.80.

(b) 15b. Yield: 109 mg (31%). IR (benzene): 3100 w, 2920 s, 2900 s, 2890 s, 2868 s, 2128 w, 2000 vs, 1955 vs, 1928 vs, 1892 s, 1865 s, 1778 s, 1755 w 1525 s, 1248 s, 935 s, 892 vs cm^{-1}. ^{1}H NMR (C_6D_6): δ 0.10 [s, Si(CH_3)$_3$], 0.97 (m, CH_3), 1.41 (m, H^d of CHH), 1.44 [m, (CH_2)^3 of ^{n}Bu], 2.15 [m, (CH_2)^2 of ^{n}Bu], 2.29 (m, H^c of CHH), 3.35 (m, H$^{b/b'}$ of CH_2N), 3.73 (m, H$^{a/a'}$of CH_2N), 4.21 [m, (CH_2)^1 of ^{n}Bu], 4.52 [s, (C_5H_5)Fe−Zr], 4.69 [s, (C_5H_5)Fe−C]. ^{13}C NMR (C_6D_6): δ 0.6 [Si(CH_3)$_3$], 14.0 (CH_3), 21.3 (C^3 of ^{n}Bu), 31.8 (C^2 of ^{n}Bu), 40.9 {CH_2[CH$_2$NSi(CH$_3$)$_3$]$_2$}, 50.1 (CH_2N), 62.8 (C^1 of ^{n}Bu), 80.9 [(C_5H$_5$)Fe−Zr], 90.2 [(C_5H$_5$)Fe−C], 215.8 [(CO)$_2$Fe−Zr], 220.2 [(CO)$_2$Fe−C], 283.4 (C═N). ^{29}Si NMR (C_6D_6): δ −1.3. Anal. Calcd for $C_{28}H_{43}Fe_2N_3O_4Si_2Zr$: C, 45.16; H, 5.82, N, 5.64. Found: C, 44.38; H, 5.78; N, 5.21.

(c) 15c. Yield: 77 mg (33%). IR (benzene): 3105 w, 2940 s, 2898 s, 2854 s, 2120 s, 1998 vs, 1952 vs, 1932 vs, 1892 s, 1880 vs, 1778 s, 1755 w, 1498 s, 1248 s, 945 s, 898 s cm^{-1}. ^{1}H NMR (C_6D_6): δ 0.12 [s, Si(CH_3)$_3$], 1.32 [br, (CH_2)^4 of Cy and H^d of CHH], 1.76, 2.14 [both m, (CH$_2$)^2 and (CH$_2$)^3], 2.27 (m, H^c of CHH), 3.35 (m, H$^{b/b'}$ of CH_2N), 3.91 (m, CH^1 and H$^{a/a'}$ of CH_2N), 4.53 [s, (C_5H_5)Fe−Zr], 4.60 [s, (C_5H_5)Fe−C]. ^{13}C NMR (C_6D_6): δ 0.9 [Si(CH_3)$_3$], 25.7 (C^4 of Cy), 26.0 (C^3 of Cy), 32.8 (C^2 of Cy), 41.0 {CH_2[CH$_2$NSi(CH$_3$)$_3$]$_2$}, 49.3 (CH_2N), 75.5 (C^1 of Cy), 80.9 [(C_5H$_5$)Fe−Zr], 90.2 [(C_5H$_5$)Fe−C], 216.8 [(CO)$_2$Fe−Zr], 219.4 [(CO)$_2$Fe−C], 282.7 (C═N). ^{29}Si NMR (C_6D_6): δ −1.1. Anal. Calcd for $C_{30}H_{45}Fe_2N_3O_4Si_2Zr$: C, 46.75; H, 5.88; N, 5.45. Found: C, 47.20; H, 5.79; N, 5.32.

(d) 15d. Yield: 107 mg (53%). ^{1}H NMR (C_6D_6): δ 0.20 [s, SiC(CH$_3$)$_3$], 1.36 (m, H^d), 2.06 (CH$_3$), 2.39 (m, H^c), 3.38 (m, H$^{b/b'}$), 3.40 (m, H$^{a/a'}$), 4.25 [(C_5H_5)Fe−Zr], 4.54 [(C_5H_5)Fe−C], 7.08 (d, H^{3,5}, $^3J_{ortho}$ = 8.00 Hz), 7.37 (d, 2 H, H^{2,6}). ^{13}C NMR (C_6D_6): δ 0.46 [SiC(CH$_3$)$_3$], 21.03 (CH$_3$), 41.07 (CH$_2$), 49.54 (CH$_2$N), 81.04 [(C_5H_5)Fe−Zr], 90.61 [(C_5H_5)Fe−C], 122.34 (C^{3,5}), 131.85 (C^{2,6}), 154.01 (C^4), 173.16 (C^1), 214.88 [(CO)$_2$Fe−Zr], 219.29 [(CO)$_2$Fe−C], 297.66 (C═N). Anal. Calcd for $C_{31}H_{41}N_3Si_2ZrFe_2O_4$: C, 47.81; H, 5.31; N, 5.40. Found: C, 48.54; H, 5.25; N, 5.69.

(e) 16a. Yield: 128 mg (67%). IR (toluene): 2895 vw, 2845 vw, 2015 vs, 1955 vs, 1942 vs, 1876 vs, 1552 w, 1418 w, 1249 m, 1110 vw, 1058 vw, 960 m, 838 s cm^{-1}. ^{1}H NMR (C_6D_6): δ 0.04 [s, Si(CH_3)$_3$], 1.47 (m, H^d of CHH), 2.39 (m, H^c of CHH), 3.34 [ddd, ^2J(H^{a}H^b) = ^2J(H$^{a'}$H$^{b'}$) = 14.0 Hz, ^3J(H^{b}H^c) = ^3J(H$^{b'}$H^c) = 5.7 Hz, ^3J(H^{b}H^d) = ^3J(H$^{b'}$H^d) = 2.9 Hz, H$^{b/b'}$ of CHHN], 3.64 [ddd, ^3J(H^{a}H^d) = ^3J(H$^{a'}$H^d) = 10.4 Hz, ^3J(H^{a}H^c) = ^3J(H$^{a'}$H^c) = 2.0 Hz, H$^{a/a'}$ of CHHN], 3.89 (s, NCH_3), 4.99 [s, (C_5H_5)Ru−Zr], 5.01 [s, (C_5H_5)Ru−C]. ^{13}C NMR (C_6D_6): δ 0.4 [Si(CH_3)$_3$], 40.8 (CH_2), 48.9 (NCH_3), 50.0 (CH_2N), 84.1 [(C_5H$_5$)Ru−Zr], 93.3 [(C_5H$_5$)Ru−C], 200.0 [(CO)$_2$Ru−C], 208.4 [(CO)$_2$Ru−Zr], 271.6 (C═N). ^{29}Si NMR (C_6D_6): δ −1.3. Anal. Calcd for $C_{25}H_{37}N_3O_4Ru_2Si_2Zr$: C, 37.86; H, 4.70; N, 5.30. Found: C, 37.68; H, 4.88; N, 5.39.

(f) 16b. Yield: 256 mg (55%). IR (benzene): 2100 w, 2950 s, 2925 s, 2890 s, 2870 s, 2820 s, 2145 w, 2020 s, 1950 vs, 1880 vs, 1787 w, 1528 s, 1246 s, 945 s, 895 vs cm^{-1}. ^{1}H NMR (C_6D_6): δ 0.08 [s, SiC(CH_3)$_3$], 0.99 (m, CH_3), 1.34 (m, H^d of CHH), 1.46 [m, (CH_2)^3], 2.11 [m, 2 H, CH$_2$)^2 of ^{n}Bu], 2.39, (m, H^c of CHH), 3.33 (m, H$^{b/b'}$ of CH$_2$N), 3.73 (m, H$^{a/a'}$of CH$_2$N), 4.18 [m, (CH$_2$)^1 of ^{n}Bu], 5.02 [s, (C_5H_5)RuZr], 5.03 [s, (C_5H_5)Ru−C]. ^{13}C NMR (C_6D_6): δ 0.61 [s, Si(CH_3)$_3$], 14.07 (CH_3), 21.35 (C^3 of ^{n}Bu), 31.86 (C^2 of ^{n}Bu), 40.58 (CH_2), 49.55 (CH_2N), 64.08 (C^1 of ^{n}Bu), 84.11 [(C_5H$_5$)Ru−Zr], 93.26 (C_5H$_5$)Ru−C], 200.62 [(CO)$_2$Ru−Zr], 208.42 [(CO)$_2$Ru−C], 271.54 (N═C). ^{29}Si NMR (C_6D_6): δ −1.55. Anal. Calcd for $C_{28}H_{43}N_3O_4Ru_2Si_2Zr$: C, 40.27; H, 5.19; N, 5.03. Found: C, 39.98; H, 5.21; N, 5.12.

(g) 16c. Yield: 136 mg (53%). IR (benzene): 3090 w, 2930 s, br, 2885 s, 2845 s, 2015 vs, 1950 vs, br, 1878 vs, 1772 s, 1510 s, 1245 s, 1090 w, 1035 s, 940 s, 895 s, 840 s, 792 s, 742 s, 730 s, 680 w, 630 w, 605 w cm^{-1}. ^{1}H NMR (C_6D_6): δ 0.09 [s, SiC(CH_3)$_3$], 1.10−1.56 [m, br, (CH_2)^4 of Cy and H^d of CHH], 1.82, 2.05−2.45 [m, br, (CH$_2$)^2, (CH$_2$)^3 of Cy, H^c of CHH], 3.31 (m, H$^{b/b'}$ of CH_2N), 3.93 (m, H$^{a/a'}$of CH_2N), 5.02 [s, (C_5H_5)Ru−Zr], 5.03 [s, (C_5H_5)Ru−CZr]. ^{13}C NMR (C_6D_6): δ 0.9 [Si(CH_3)$_3$], 25.7 (C^4 of Cy), 26.0 (C^3 of Cy), 32.9 (C^2 of Cy), 40.8 [CH_2(CH$_2$NSiMe$_3$)$_2$], 48.7 (CH$_2$N), 76.1 (C^1 of Cy), 84.2 [(C_5H$_5$Ru−Zr], 93.4 [(C_5H$_5$)Ru−C], 200.8 [(CO)$_2$Ru−Zr], 208.1 [(CO)$_2$Ru−C], 270.8 (C═N). ^{29}Si NMR (C_6D_6): δ = −1.3 (s). Anal. Calcd for $C_{30}H_{45}N_3O_4Ru_2Si_2Zr$: C, 41.84; H, 5.27; N, 4.88. Found: C, 42.34; H, 5.35; N, 4.85.

(h) 16d. Yield: 171 mg (64%). IR (benzene): 2960 w, 2930 w, 2895 w, 2850 w, 2025 vs, 1965 vs, 1945 vs, 1875 vs, 1530 w, 1245 s, 1025 vw, 1008 vw, 930 w, 898 s, 831 s, 810 s, 798 s, 765 w, 742 w, 615 vw cm^{-1}. ^{1}H NMR (C_6D_6): δ 0.18 [s, Si(CH_3)$_3$], 1.39 (m, 1 H^d of CH_2], 2.1 (s, Ar−CH$_3$), 2.47 (m, H^c of CH_2), 3.37 [ddd, H$^{b/b'}$, ^2J(H^{a}H^b) = ^2J(H$^{a'}$H$^{b'}$) = 14.26 Hz, ^3J(H^{b}H^c) = ^3J(H$^{b'}$H^c) = 5.3 Hz, ^3J(H^{b}H^d) = ^3J(H$^{b'}$H^d) = 2.93 Hz, ^2J(H^{c}H^d) = 10.97 Hz, CH_2N), 3.96 [ddd, 2 H, H$^{a/a'}$, ^3J(H^{a}H^d) = ^3J(H$^{a'}$H^d) = 10.78 Hz, ^3J(H^{a}H^c) = ^3J(H$^{a'}$H^c) 2.93 Hz, CH_2N], 4.76 [s, 5 H, (C_5H_5)Ru−Zr], 4.95 (s, 5 H, (C_5H_5)Ru−C], 7.11 (d, 2 H, H-2, ^3J(H^{2}H^3) = 8.1 Hz), 7.36 (d, 2 H, H^3). ^{13}C NMR (C_6D_6): δ 0.92 [SiC(CH$_3$)$_3$], 20.98 (Ar−CH_3), 40.78 [CH$_2$(CH$_2$NSiMe$_3$)$_2$], 49.04 (CH_2N), 84.17 [(C_5H$_5$)Ru−Zr], 93.40 [(C_5H$_5$)Ru−C], 122.15 (C^3 of *p*-Tol), 129.93 (C^2 of *p*-Tol), 135,73 (C^4 of *p*-Tol), 155.70 (C^1 of *p*-Tol), 199.75 [(CO)$_2$Ru−Zr], 208.00 [(CO)$_2$Ru−C], 284.47 (C−Zr). ^{29}Si NMR (C_6D_6): δ −0.72 (s). Anal. Calcd for $C_{31}H_{41}N_3O_4Ru_2Si_2Zr$: C, 42.84; H, 4.75; N, 4.83. Found: C, 43.02; H, 4.72; N, 4.79.

(11) Preparation of [CH$_2$(CH$_2$NSiMe$_3$)$_2$Zr{[μ-κ^2(*O*,*O*):κ^1(*C*)]-[Fe(SMeR)(CO)$_2$Cp]$_2$}] (R = Me, Ph, Tol (17a−c)). To a stirred solution of CH$_2$(CH$_2$NSiMe$_3$)$_2$Zr[Fe(CO)$_2$Cp]$_2$ (**2**) (160 mg = 0.242 mmol) in 5 mL of benzene was added 0.484 mmol of sulfoxide (Me$_2$SO, PhMeSO, TolMeSO). The reaction mixture was stirred for 2 min, and the solvent was carefully removed in vacuo, yielding an orange solid which contained a mixture of the diastereomers of **17a**−**c**.

(a) 17a. Yield: 48 mg (24%). IR (benzene): 2947 s, 2915 s, w, 1949 vs, 1783 w, 1255s, 1248 s, 1089 vw, 1054 vw, 982 vw, 957 vw,

830 vs, 800 s, 746 w cm^{-1}. ^1H NMR (C_6D_6): δ 0.44 [Si(CH_3)$_3$], 1.68−1.91 [m, br, S−CH_3 and CH_2(CH$_2$NSiMe$_3$)$_2$], 3.74 (m, CH_2N), 4.28 (s, C$_5H_5$), 4.29 (s, C$_5H_5$). ^{13}C NMR (C_6D_6): δ 1.4 [Si(*C*H$_3$)$_3$], 25.9 (S−*C*H$_3$), 26.0 (S−*C*H$_3$), 34.9 [*C*H$_2$(CH$_2$NSiMe$_3$)$_2$], 45.2 (*C*H$_2$N meso), 45.3 (*C*H$_2$N rac), 45.4 (*C*H$_2$N meso), 83.7 (*C*$_5$H$_5$), 83.8 (*C*$_5$H$_5$), 219.8 (*C*O), 248.8 (*C*O$_2$), 249.0 (*C*O$_2$). Anal. Calcd for $C_{27}H_{46}Fe_2N_2O_6S_2Si_2Zr$: C, 39.65; H, 5.67; N, 3.43. Found: C, 39.84; H, 5.63; N, 3.35.

(b) 17b. Yield: 58 mg (26%). IR (benzene): 3045 w, 2940 s, 2915 s, 2885 s, 2840 w, 2150 vw, 1989 s, sh, 1941 vs, br, 1772 s, sh, 1725 vw, 1242 vs, br, cm^{-1}. ^1H NMR (C_6D_6): δ = 0.52 [s, Si(CH_3)$_3$], 1.86 [CH_2(CH$_2$NSiMe$_3$)$_2$], 2.35 (s, 3 H, SCH_3), 2.36 (s, SCH_3), 3.80 (CH_2N), 4.24 (s, C$_5H_5$). ^{13}C NMR (C_6D_6): δ = 1.4 [Si(*C*H$_3$)$_3$], 26.0 [*C*H$_2$(CH$_2$NSiMe$_3$)$_2$], 39.6 (S−*C*H$_3$), 39.8 (S−*C*H$_3$), 45.7 (*C*H$_2$N meso), 45.8 (*C*H$_2$N rac), 84.2 (*C*$_5$H$_5$), 84.4 (*C*$_5$H$_5$), 129.4 (C^3), 129.6 (C^2), 139.2 (C^4), 140.1 (C^1), 219.9 (CO), 247.8 (*C*O$_2$), 247.9 (*C*O$_2$). Anal. Calcd for $C_{37}H_{50}Fe_2N_2O_6S_2Si_2Zr$: C, 47.18; H, 5.35; N, 2.97. Found: C, 47.32; H, 5.39; N, 2.99.

(c) 17c. Yield: 58 mg (26%). IR (benzene): 2940, 2919, 2888 s, 2843 w, 2130 vw, 1990 vs, 1942 vs, br, 1770 vs, 1490 s, sh, 1247 vs cm^{-1}. ^1H NMR (C_6D_6): δ 0.51 [s, Si(CH_3)$_3$], 1.85 [m, CH_2(CH$_2$NSiMe$_3$)$_2$], 2.00 (s, *p*-Tol CH_3), 2.38 and 2.39 (s, S−CH_3), 3.81 (t, CH_2N), 4.28 (s, C$_5H_5$), 6.85 [d, ^3J(H^{2}H^3) = 8.0 Hz, H^3], 7.36 (d, H^2). ^{13}C NMR (C_6D_6): δ 1.4 [Si(*C*H$_3$)$_3$], 20.8 (*p*-Tol *C*H$_3$), 21.0 (*p*-Tol *C*H$_3$), 26.3 (S−*C*H$_3$), 35.3 [*C*H$_2$(CH$_2$NSiMe$_3$)$_2$], 45.7 (*C*H$_2$N), 84.3 (*C*$_5$H$_5$), 129.8 (C^3), 130.0 (C^3), 136.6 (C^4), 138.7 (C^1), 220.0 (*C*O), 248.3 (*C*O$_2$). Anal. Calcd for $C_{39}H_{54}Fe_2N_2O_4S_2Si_2Zr$: C, 48.29; H, 5.61; N, 2.89. Found: C, 48.35; H, 5.55; N, 2.78.

(12) Preparation of [CH$_2$(CH$_2$NSiMe$_3$)$_2$Zr{[μ-κ^2(*O*,*O*):κ^1(*C*)]-[Ru(SMeR)(CO)$_2$Cp]}$_2$] (R = Me, Ph, Tol (18a−c)). To a stirred solution of CH$_2$(CH$_2$NSiMe$_3$)$_2$Zr[Ru(CO)$_2$Cp]$_2$ (320 mg = 0.425 mmol) in 5 mL of benzene was added 0.850 mmol of sulfoxide [Me$_2$SO, Ph(Me)SO, Tol(Me)SO] with the aid of a microliter syringe. After the solution was stirred at ambient temperature for ca. 2 min, the solvent was carefully removed in vacuo. A yellow-orange powder was obtained containing **18a−c** as a mixture of the two diastereomers.

(a) 18a. Yield: 61%. IR (benzene): 2940 s, 2910 s, 2840 w, 1940 vs, 1775 vw, 1422 s, 1345 s, 1247 vs, br, 1090 vw, 1055 vw, 980 vw, 955 vw, 828 vs, 798 s, 745 w cm^{-1}. ^1H NMR (C_6D_6): δ 0.46 [s, Si(CH_3)$_3$], 1.79 [m, CH_2(CH$_2$NSiMe$_3$)$_2$], 2.10 (s, SMe$_2$), 3.74 (m, CH_2N), 4.72 (s, C$_5H_5$), 4.74 (s, C$_5H_5$). ^{13}C NMR (C_6D_6): δ = 1.5 [Si(*C*H$_3$)$_3$], 28.5 (SMe$_2$), 28.6 (SMe$_2$), 34.9 [*C*H$_2$(CH$_2$NSiMe$_3$)$_2$], 35.0 [*C*H$_2$(CH$_2$NSiMe$_3$)$_2$], 45.2 (*C*H$_2$N meso), 45.4 (*C*H$_2$N rac), 45.8 (*C*H$_2$N meso), 86.8 (*C*$_5$H$_5$), 86.9 (*C*$_5$H$_5$), 204.5 (*C*O), 204.6 (*C*O), 231.4 (*C*O$_2$), 231.6 (*C*O$_2$). ^{29}Si NMR (C_6D_6): δ −0.8 (s, meso), −0.7 (s, rac), −0.6 (s, meso). Anal. Calcd for $C_{27}H_{46}N_2O_6Ru_2S_2Si_2Zr$: C, 35.70; H, 5.10; N, 3.08. Found: C, 35.93; H, 5.21; N, 3.05.

(b) 18b. Yield: 60%. IR (benzene): 3050 w, 2940, w, 2920 w, 2890 w, 2845 w, 1952 vs, 1375 s, 1290 vs, 1110 w, 1075 w, 985 w, 765 s cm^{-1}. ^1H NMR (C_6D_6): δ 0.49 [s, Si(CH_3)$_3$], 1.84 [m, 2 H, CH_2(CH$_2$NSiMe$_3$)$_2$], 2.65 and 2.67 (s, SCH_3), 3.78 (m, CH_2N), 4.65 and 4.66 (both s, C$_5H_5$). ^{13}C NMR (C_6D_6): δ 1.5 [Si(*C*H$_3$)$_3$], 28.2 and 28.3 (S−*C*H$_3$), 35.3 [*C*H$_2$(CH$_2$NSiMe$_3$)$_2$], 45.7 (*C*H$_2$N), 87.3 (*C*$_5$H$_5$), 128.6 (C^4), 129.1 (C^3), 129.2 (C^2), 141.0 (C^1), 204.5 (*C*O), 230.4 and 230.5 (*C*O$_2$). ^{29}Si NMR (C_6D_6): δ −0.6 (s). Anal. Calcd for $C_{37}H_{50}N_2O_6S_2Si_2Ru_2Zr$: C, 43.04, H, 4.88; N, 2.71. Found: C, 42.57; H, 4.65; N, 2.55.

(c) 18c. Yield: 63%. IR (benzene): 2945 w, 2925 w, 2895 w, 2840 w, 1950 vs, sh, 1348 w, 1258 vs, 1096 s, 1050 s, 1005 s, 830 s, 795 s cm^{-1}. ^1H NMR (C_6D_6): δ 0.51 [s, Si(CH_3)$_3$], 1.85 [m, CH_2(CH$_2$NSiMe$_3$)$_2$], 2.00 (SCH_3), 2.70 (*p*-Tol CH_3), 2.71 (*p*-Tol CH_3), 3.79 (m, CH_2N), 4.69 (s, C$_5H_5$), 4.70 (s, C$_5H_5$). ^{13}C NMR (C_6D_6): δ 1.5 [Si(*C*H$_3$)$_3$], 20.9 (S*C*H$_3$), 28.6 (*p*-Tol *C*H$_3$), 28.7 (*p*-Tol *C*H$_3$), 35.3 [*C*H$_2$(CH$_2$NSiMe$_3$)$_2$], 45.7 (*C*H$_2$N), 87.4 (*C*$_5$H$_5$), 87.3 (*C*$_5$H$_5$), 129.4 (C^3), 129.6 (C^2), 137.6 (C^4), 138.7 (C^1), 138.8 (C^1), 204.5 (*C*O), 230.9 (*C*O$_2$), 230.8 (*C*O$_2$). ^{29}Si NMR (C_6D_6): δ −0.6. Anal. Calcd for $C_{39}H_{54}N_2O_6Ru_2S_2Si_2Zr$: C, 44.17; H, 5.13; N, 2.64. Found: C, 43.99; H, 5.10; N, 2.63.

(13) X-ray Crystallographic Study of 1, 2, 3, 9, and 16a. (a) Data Collection for 1, 2, 3, 9, and 16a. Crystals of **1**, **2**, **3**, **9**, and **16a** were mounted on a quartz fiber in Lindemann capillaries under argon and in an inert oil. X-ray intensity data were collected with graphite-monochromated radiation, on a Siemens P4 four-circle diffractometer for **1**, **3**, **9**, and **16a** and on a Philips PW1100 four-circle diffractometer for **2**. Details of data collection and refinement and crystal data are listed in Table 1. Lorentz−polarization and absorption corrections were applied to the data of all the compounds.

(b) Structure Solution and Refinement for 1, 2, 3, 9, and 16a. For compound **2**, the positions of the three metal atoms were deduced from a Patterson synthesis, and for **1**, **3**, **9**, and **16a**, the positions of most of the non-hydrogen atoms were located by direct methods. The remaining non-hydrogen atoms were revealed from subsequent difference Fourier syntheses. In the isomorphous structures of **2** and **3**, there was slight conformational disorder of the propyl chains, C(7) of each structure being resolved into two components in a 60:40% ratio; in **16a**, rotational disorder of one cyclopentadienyl group meant that partial atoms (0.7:0.3 occupancy) at two sites were refined for each atom of ring C(22)−C(26). For **2**, refinement was based on *F*,[44] and for the other four structures, refinement was based on F^2.[45] The hydrogen atoms of the cyclopentadienyl rings were not included in structure factor calculations except those in **2**, which were located directly and were included but not refined. All other hydrogen atoms were placed in calculated positions with displacement parameters fixed at a value of 0.08 Å^2 in **2**, and set equal to 1.2U_{eq} or 1.5U_{eq} of the parent carbon atoms for the methylene and methyl groups in the other four structures. Semiempirical absorption corrections[45] using ψ-scans were applied to the data of **1**, **9**, and **16a**, and after initial refinement with isotropic displacement parameters, empirical absorption corrections[46] were applied to the data of **2** and **3**. All full-occupancy non-hydrogen atoms were assigned anisotropic displacement parameters in the final cycles of full-matrix least-squares refinement.

Results and Discussion

The starting material for the synthesis of the heterobimetallic complexes was the previously reported amidozirconium complex [CH$_2$(CH$_2$NSiMe$_3$)$_2$ZrCl$_2$(thf)$_2$],[13] and during the course of the present work, X-ray-quality crystals were obtained. Since the configuration of the hexacoordinate compound could not be established unambiguously by spectroscopic techniques [ν(Zr−Cl) bands were obscured by other vibrations in the IR spectrum], a single-crystal X-ray structure analysis was carried out which proved that our previous structural proposal[13] based on a cis arrangement of the chloro ligands was incorrect and established the trans disposition of the two Cl ligands. We therefore briefly present the results of the X-ray diffraction experiment which has established the trans disposition of the two Cl ligands. (See Chart 2.)

Crystal Structure Analysis of [CH$_2$(CH$_2$NSiMe$_3$)$_2$ZrCl$_2$-(thf)$_2$] (1). Single crystals of compound **1** suitable for X-ray crystallography were obtained from a concentrated solution in THF at −30 °C. The structure analysis revealed a distorted octahedral molecular geometry with the chloro ligands trans to each other (Figure 1). The molecule has crystallographic C_2 symmetry with the symmetry axis aligned along the vector connecting the Zr atom and C(8) of the ligand backbone, the ligand adopting a symmetrical twisted conformation [Zr, N(1), N(2), and C(8) exactly coplanar] as shown in Figure 1b with the Me$_3$Si groups on opposite sides of the chelate ring. The significant deviation from the octahedral symmetry is reflected in the Cl(1)−Zr−Cl(2) angle of 160.33(6)°. The minimum contact distance between the chloro and bidentate ligands is Cl(1)···H(methyl) = 2.91 Å (cf. sum of van der Waals radii 2.95 Å), and without the distortion of the axial Cl ligands away

(44) Sheldrick, G. M. SHELX 76: Program for Crystal Structure Determination. University of Cambridge, 1976.
(45) *SHELTXL*, PC version 5.03; Siemens Analytical Instruments Inc.: Madison, W1, 1994.
(46) Walker, N.; Stuart, D. *Acta Crystallogr., Sect. A* **1983**, *39*, 158.

Table 1. Crystal Data and Structure Refinement Parameters for Complexes **1**, **2**, **3**, **9**, and **16a**

	1	**2**	**3**
empirical formula	$C_{17}H_{40}Cl_2N_2O_2Si_2Zr$	$C_{23}H_{34}N_2O_4Fe_2Si_2Zr$	$C_{23}H_{34}N_2O_4Ru_2Si_2Zr$
fw	522.81	661.52	752.06
crystal system	monoclinic	monoclinic	monoclinic
space group	*C*2/*c* (No. 15)	$P2_1/n$ (alt. No. 14)	$P2_1/n$ (alt. No. 14)
a, Å	20.710(2)	11.333(2)	11.3944(9)
b, Å	10.8962(12)	13.001(3)	13.196(2)
c, Å	11.7166(13)	19.364(4)	19.5280(14)
β, deg	102.703(7)	96.58(2)	96.191(5)
V, Å^3	2579.3(4)	2834.3(2)	2919.1(6)
Z	4	4	4
ρ_{calc}, Mg m^{-3}	1.346	1.551	1.711
radiation (λ, Å)	Mo Kα (0.710 73)	Mo Kα (0.710 69)	Cu Kα (1.541 78)
μ, min^{-1}	0.740	1.490	12.181
final *R* indices[a]			
$I > 2\sigma(I)$	$R_1 = 0.0475$, w$R_2 = 0.0844$	$R = 0.0555$, $R' = 0.0550$*	$R_1 = 0.0379$, w$R_2 = 0.1413$
all data	$R_1 = 0.0956$, w$R_2 = 0.0993$		$R_1 = 0.0432$, w$R_2 = 0.2808$
weights: *a*, *b*[a]	0.0574, 4.3357	b	0.0450, 6.9954
max and min $\Delta\rho$, e Å^{-3}	0.306 and −0.313	0.538 and −0.522	1.048 and −1.035

	9	**16a**
empirical formula	$C_{21}H_{34}N_2O_2RuSi_2Zr$	$C_{25}H_{37}N_3O_4Ru_2Si_2Zr$
fw	594.97	793.12
crystal system	monoclinic	monoclinic
space group	$P2_1/c$ (No. 14)	$P2_1/c$ (No. 14)
a, Å	10.477(2)	10.8252(9)
b, Å	26.883(4)	13.0511(9)
c, Å	9.9960(12)	13.089(2)
β, deg	113.113(14)	95.720(6)
V, Å^3	2589.3(7)	3245.8(4)
Z	4	4
ρ_{calc}, Mg m^{-3}	1.526	1.623
radiation (λ, Å)	Cu Kα (1.541 78)	Mo Kα (0.710 73)
μ, mm^{-1}	9.053	1.339
final *R* indices[a]		
$I > 2\sigma(I)$	$R_1 = 0.0674$, w$R_2 = 0.1700$	$R_1 = 0.0335$, w$R_2 = 0.0764$
all data	$R_1 = 0.0981$, w$R_2 = 0.2168$	$R_1 = 0.0531$, w$R_2 = 0.0882$
weights: *a*, *b*[a]	0.0890, 26.6043	0.0343, 4.6990
max and min $\Delta\rho$, e Å^{-3}	1.681 and −0.977	0.545 and −0.383

[a] $S = [\sum w(F_o^2 - F_c^2)^2/(n - p)]^{1/2}$ where n = number of reflections and p = total number of parameters; $R_1 = \sum||F_o| - |F_c||/\sum|F_o|$, w$R_2 = \sum[w(F_o^2 - F_c^2)^2]/\sum[w(F_o^2)^2]^{1/2}$, $w^{-1} = [\sigma^2(F_o)^2 + (aP)^2 + bP]$, $P = [\max(F_o^2, 0) + 2(F_c^2)]/3$. [b] For **2**, weights of $1/\sigma^2(F)$ were applied [$I/\sigma(I) > 3$]; $R = \sum(\Delta F)/\sum(F_o)$; $R' = [\sum(\Delta F)^2/\sum w(F_o)^2]^{1/2}$.

Chart 2

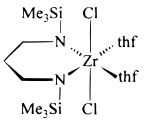

from the bidentate ligand, this would be unfavorably short. The displacement of the chlorine atoms toward the two symmetry-related thf ligands also facilitates the formation of hydrogen bonds with two methylene hydrogen atoms [Cl(1)···H(C4S) 2.68 A]. All other metric parameters are unexceptional and lie within the range of values for previously reported zirconium complex structures.[47]

Synthesis and Structural Characterization of the Heterotrinuclear Complexes [CH$_2$(CH$_2$NSiMe$_3$)$_2$Zr{M(CO)$_2$Cp}$_2$] (M = Fe (2), Ru (3)) and [CH$_2$(CH$_2$NSiMe$_3$)$_2$Zr{Co(CO)$_3$PPh$_3$}$_2$] (4). Reaction of the complex [CH$_2$(CH$_2$NSiMe$_3$)$_2$ZrCl$_2$(thf)$_2$] (**1**) with 2 molar equiv of the carbonylmetalates K[MCp(CO)$_2$] (M = Fe, Ru) and Na[Co(CO)$_3$(PPh$_3$)] yielded the corresponding trinuclear compounds [CH$_2$(CH$_2$NSiMe$_3$)$_2$Zr{M(CO)$_2$Cp}$_2$] (M = Fe (**2**), Ru (**3**)) and [CH$_2$(CH$_2$NSiMe$_3$)$_2$Zr{Co(CO)$_3$PPh$_3$}$_2$] (**4**) (Scheme 1).

While both **2** and **3** are stable in solution (the latter even upon brief exposure to air), the ZrCo$_2$ complex **4** decomposes over a period of several hours, generating the brown cobalt dimer [Co(CO)$_3$(PPh$_3$)]$_2$ as well as an intractable Zr-containing material. The existence of metal−metal bonds in **2**−**4** was initially deduced from the infrared spectra, in which the ν(CO) bands are shifted to higher wavenumbers relative to those of the alkali metal salts used in the synthesis. The shift to higher frequency $\Delta\nu(CO)_{as}$ of the asymmetric ^{12}C−O stretching vibration in compounds containing the {MCp(CO)$_2$} fragment upon formation of the metal−metal bond may be used as a measure of the acceptor strength of the Lewis acidic metal fragment in relation to the base [MCp(CO)$_2$]$^-$ (M = Fe, $\nu(CO)_{as}$ = 1770 cm^{-1}; M = Ru, $\nu(CO)_{as}$ = 1811 cm^{-1} (for the K$^+$ salt)).[48] It is interesting to compare the position of the asymmetric ^{12}C−O stretching vibration of **3** with that of [Cp$_2$Zr{RuCp(CO)$_2$}$_2$];[7] for **3**, the value of $\Delta\nu(CO)_{as}$ was found to be 97 cm^{-1} while the value for Casey's Cp$_2$ZrRu$_2$ compound is only 71 cm^{-1}. The greater Lewis acidity of the amidozirconium fragment in comparison to that of the {Cp$_2$Zr} unit apparently induces a higher degree of charge redistribution from the late transition metal to the early transition metal through the metal−metal bond which therefore assumes a more covalent character.

There is also a possibility that this situation is a consequence of the different steric situation at the diamidozirconium unit in

(47) Cambridge Structural Data Base, Cambridge, U.K., 1998.

(48) Fischer, R. A.; Priermeier, T. *Organometallics* **1994**, *13*, 4306 and references cited therein.

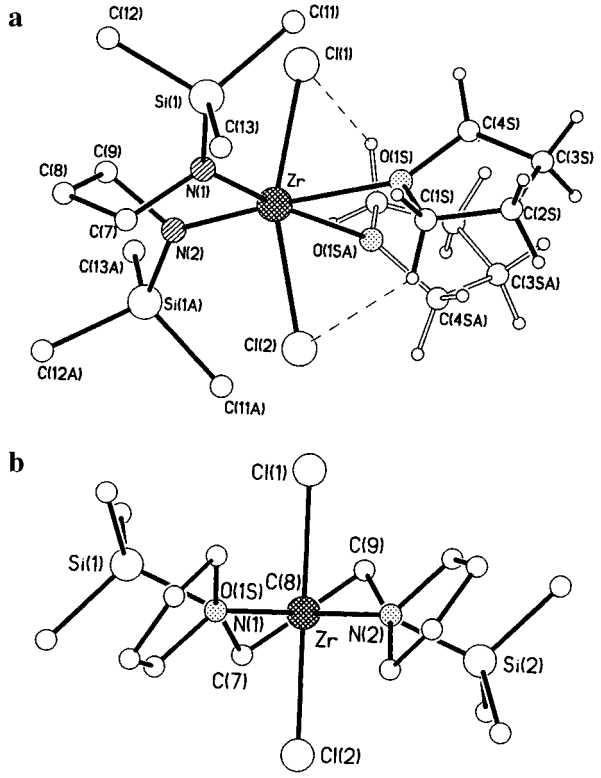

Figure 1. Views of the molecular structure of $[CH_2(CH_2NSiMe_3)ZrCl2(thf)_2]$ (**1**) which has exact C_2 symmetry: (a) view showing the hydrogen-bonding between the thf and the chloro ligands; (b) view along the C_2 axis showing the conformation of the chelate ring [N(1) lies behind O(1S)]. The principal bond lengths and angles are listed in Table 2, and for ease of comparison, the symmetry equivalents of atoms Cl(1), Si(1), N(1), and C(7) (at $-x$, y, $0.5 - z$) have been assigned labels Cl(2), Si(2), N(2), and C(9), respectively; all other symmetry-related atoms have the same label as the original atom plus the additional letter A.

Scheme 1. Synthesis of the ZrM_2 Heterobimetallic Complexes **2**−**4**

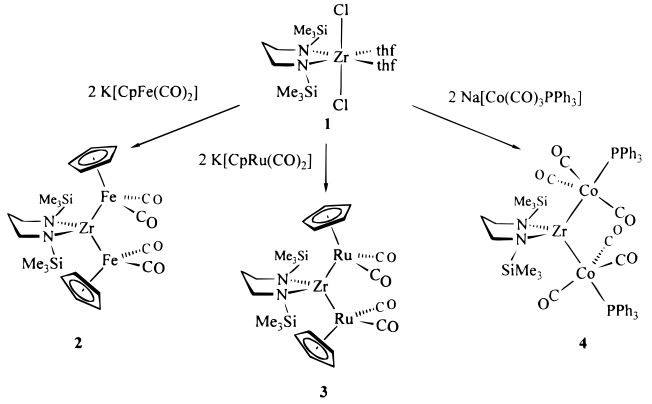

comparison to that of $\{Cp_2Zr\}$. In fact, we expected this difference in the IR spectroscopic data to be reflected in the molecular structures of the compounds. To establish such a relationship and to structurally characterize a $ZrFe_2$ species for the first time, single-crystal X-ray structure analyses of **2** and **3** were carried out. The molecular structures of both compounds are depicted in Figure 2, and the principal bond lengths and interbond angles are listed in Table 2.

The crystals of the two compounds are isomorphous, and their gross structural features are identical. In each, the central zirconium atom adopts a distorted tetrahedral coordination geometry [**2**, N(1)−Zr−N(2) 97.6(3), Fe(1)−Zr-Fe(2) 116.2(1)°;

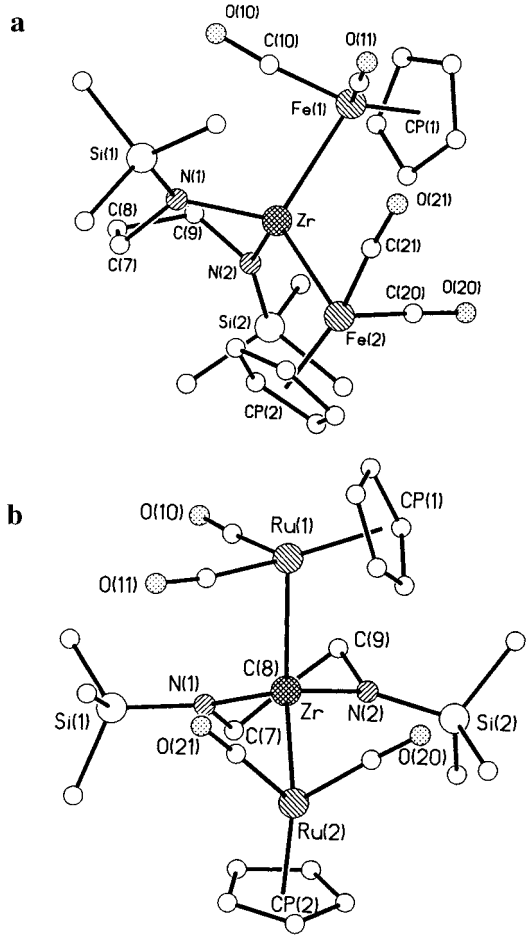

Figure 2. Isostructural molecules of the trinuclear compounds $[CH_2(CH_2NSiMe_3)_2Zr\{M(CO)_2Cp\}_2]$ (**2**, (**3**) illustrated by (a) a view of **2** (M = Fe) showing the conformation of the chelate ring and (b) a view of **3** (M = Ru) along the Zr···C(8) vector showing the conformation of the major component. The principal bond lengths and angles for both compounds are listed in Table 2.

3, N(1)−Zr−N(2) 97.6(2), Ru(1)−Zr−Ru(2) 115.84(2)°] and links to the iron or ruthenium complex fragments through direct unsupported metal−metal bonds. The Zr−Fe distances in the trinuclear complex **2**, Zr−Fe(1) 2.665(2) and Zr−Fe(2) 2.664(2) Å, lie in the range between that in a dinuclear complex of the same ligand $[CH_2(CH_2NSiMe_3)_2(Cp)Zr{-}FeCp(CO)_2]$ of 2.745(1) Å[41] and that of 2.605(2) Å in the tripodamide complex $[MeSi\{SiMe_2N(4\text{-}CH_3C_6H_4)\}_3Zr{-}FeCp(CO)_2]$.[20] The Zr−Ru bond lengths in **3** [Zr−Ru(1) 2.7372(7) and Zr−Ru(2) 2.7452(7) Å] are much shorter than the those of 2.9381(1) and 2.948(1) Å in $[Cp_2Zr\{RuCp(CO)_2]$[24] and of 2.910(1) Å in $[Cp_2(O^tBu)Zr{-}RuCp(CO)_2]$,[24] the two Zr−Ru heterobimetallics containing $\{Cp_2Zr\}$ fragments reported by Casey and co-workers. In Casey's compound, the steric congestion around the zirconium centers is probably important in determining the metal−metal bond lengths.

A direct relationship between the metal−metal distance in early late heterobimetallic complexes and the nature of the bonding interaction was deduced by Wolczanski et al. in an early Extended Hückel MO study of various Zr-M complexes known at the time.[50] In particular, the degree of metal−metal

(49) Casey, C. P.; Jordan, R. F.; Rheingold, A. L. *J. Am. Chem. Soc.* **1983**, *105*, 665.
(50) Ferguson, G. S.; Wolczanski, P. T.; Parkanyi, L.; Zonnevylle, M. *Organometallics* **1988**, *7*, 1967.

Table 2. Selected Bond Lengths and Angles for the Dichloride **1**, the Trinuclear Compounds **2** and **3**, the Dinuclear Compound **9**, and the Trinuclear Insertion Product **16a**

	1 $ZrCl_2$	**2** $ZrFe_2$	**3** $ZrRu_2$	**9** ZrRu	**16a** $ZrRu_2$
			(a) Lengths (Å)		
Zr−M(1)/Cl(1)	2.489(1)	2.665(2)	2.7372(7)	2.828(1)	2.8639(6)
Zr−M(2)/Cl(2)	2.489(1)	2.664(2)	2.7452(7)		
Zr−N(1)	2.039(4)	2.039(7)	2.042(5)	2.045(11)	2.066(4)
Zr−N(2)	2.039(4)	2.040(7)	2.025(5)	2.044(1)	2.025(4)
Zr−O(1S)	2.368(3)				
Zr−Cp(2)[a]				2.249(11)	
M(1)−Cp(1)[a]		1.726(10)	1.927(8)	1.939(15)	1.941(8)
M(2)−Cp(2)[a]		1.736(10)	1.935(7)		1.94(1)
M(1)−C(10)		1.722(10)	1.851(8)	1.763(14)	1.858(6)
M(1)−C(11)		1.721(11)	1.857(9)	1.842(16)	1.835(6)
M(2)−C(20)		1.716(11)	1.841(8)		1.866(6)
M(2)−C(21)		1.715(12)	1.846(7)		1.865(6)
Si(1)−N(1)	1.742(4)	1.742(8)	1.739(5)	1.763(12)	1.739(4)
Si(2)−N(2)	1.742(4)	1.728(8)	1.739(5)	1.727(11)	1.733(4)
N(1)−C(7)	1.500(5)	1.537(17)[b]	1.493(11)[b]	1.517(16)	1.482(6)
N(2)−C(9)	1.500(5)	1.512(12)	1.493(8)	1.472(16)	1.492(6)
			(b) Angles (deg)		
M(1)−Zr−M(2)		116.2(1)	115.84(2)		
Cl(1)−Zr−Cl(2)	160.33(6)				
N(1)−Zr−M(1)/Cl(1)	96.31	111.8(2)	113.2(1)	111.6(3)	107.1(1)
N(2)−Zr−(M1)/Cl(1)		106.2(2)	105.4(1)	107.5(3)	107.9(1)
O(1S)−Zr−Cl(1)	81.99(8)				
N(1)−Zr−M(2)/Cl(2)	97.18(11)	111.l5(2)	111.2(1)		
N(2)−Zr−M(2)/Cl(2)	96.31(11)	111.9(2)	112.1(1)		
M(1)−Zr−Cp(2)/CN[a]				114.2(3)	112.3(2)
N(1)−Zr−Cp(2)/CN[a]				115.9	117.2(2)
N(2)−Zr−Cp(2)/CN[a]				110.8	111.0(2)
N(1)−Zr−N(2)	93.1(2)	97.6(3)	97.6(2)	94.9(4)	100.5(2)
O(1S)−Zr−O(1S[i])	78.3(2)				
Zr−M(1)−Cp(1)[a]		115.4(4)	113.5(2)	115.3(4)	119.1(1)
Zr−M(1)−C(10)	84.3(4)	81.7(2)	84.6(4)	83.4(2)	
Zr−M(1)−C(11)	93.0(4)	91.5(2)	87.3(4)	78.8(2)	
Zr−M(2)−Cp(2)[a]		114.7(4)	112.8(3)		
Zr−M(2)−C(20)	89.0(4)	88.8(2)			
Zr−M(2)−C(21)	89.4(4)	89.2(2)			
C(10)−M(1)−Cp(1)[a]		129.0(5)	132.5(4)	131.6(6)	131.8(2)
C(11)−M(1)−Cp(1)[a]		128.2(5)	130.4(4)	130.4(6)	133.1(2)
C(10)−M(1)−C(11)		93.6(5)	90.0(3)	91.8(7)	90.6(2)
C(20)−M(2)−Cp(2)[a]		129.7(4)	131.8(3)		128.9(3)
C(21)−M(2)−Cp(2)[a]		129.7(4)	132.2(3)		125.8(3)
C(20)−M(2)−C(21)		92.4(5)	88.1(4)		91.2(3)
Zr−N(1)−Si(1)	138.1(2)	133.7(4)	132.4(3)	134.5(6)	126.5(2)
Zr−N(1)−C(7)	108.4(3)	110.3(7)	109.2(5)[a]	112.6(8)	119.4(3)
Si(1)−N(1)−C(7)	113.5(3)	114.4(7)	117.4(5)[a]	112.4(8)	113.7(3)
Zr−(N2)−Si(2)	138.1(2)	145.8(4)	144.9(3)	147.7(6)	134.7(2)
Zr−N(2)−C(9)	108.4(3)	102.4(6)	102.8(4)	94.2(8)	109.8(3)
Si(2)−N(2)−C(9)	113.5(3)	111.7(6)	112.2(4)	117.0(8)	115.4(3)
Zr−N(30)−C(31)					115.1(3)

[a] Midpoints of relevant atoms used. [b] Major component.

π-bonding, and thus the degree of charge relocalization, is critically determined by the Zr-M bond length. The higher wavenumbers of the ν(CO) IR bands in the amido complexes compared to the Cp_2Zr derivatives is thus manifested in their structural data (vide supra). Whereas Wolczanski's interpretation of the metal−metal bonding was also supported by the results of a Fenske−Hall MO study we published in 1996,[21] the most recent analysis of the metal−metal bond in Ti−Co and Zr−Co complexes based on modern DFT calculations has led us to consider fairly low covalent bond orders (<1) for the highly polar metal−metal bonds.[22] The detailed "mechanism" of the charge redistribution upon formation of the Zr-M bonds is thus at present not unambiguously established and the focus of further theoretical studies.

The conformation of each of the major component chelate rings in **2** and **3** (Figure 2b) is rather similar to that in **1** (some unresolved disorder in the chelate ring atoms in **2** and **3** precludes detailed discussion); however, major distortions of exo-ring angles are observed as the ligands adapt to accommodate the bulky $MCp(CO)_2$ groups. The geometry at the nitrogen is virtually planar in all three compounds [mean sum of angles at N: 360(1)° for **1**, 359(1)° for **2** and **3**]. In the precursor **1**, the Zr−N(1)−Si(1) and Zr−N(2)−Si(2) angles are equal by symmetry and have the large value of 138.1(2)°, reflecting the steric requirements of the bulky $SiMe_3$ substituents; for the trinuclear compounds, the corresponding angles are 133.7(4) and 145.8(4)° in **2** and 132.4(3) and 144.9(3)° in **3**. The extremely large angles at N(2) in **2** and **3** prevent unfavorably short contacts with the bulky Cp(1) rings; the "gauche" arrangement of the two Cp rings relative to the M(1)···M(2) vector in each compound allows the relatively smaller angles at N(1), Cp(2) being remote from $Si(1)Me_3$.

The reduction of the steric congestion around the Zr center upon replacement of the Cp_2Zr unit by the diamidozirconium

Scheme 2. Complex Fragment Redistribution upon Reacting **2** and **3** with the Dichloro Complex **1** Yielding the Dinuclear Species **5** and **6**

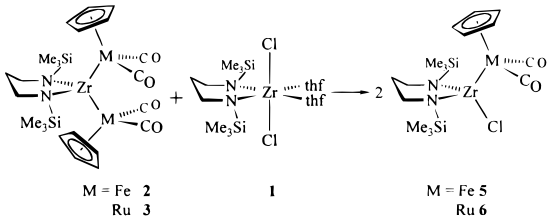

fragment employed in this work is reflected in the rapid internal rotation around the Zr−M bonds on the NMR time scale, conferring effective C_S symmetry upon the molecules in solution. In contrast to Casey's observation for $[Cp_2Zr\{RuCp(CO)_2\}_2]$, in which the internal rotation around the Zr−Ru axis could be frozen out at 180 K,[24] the ^{1}H and ^{13}C NMR spectral data for **2** and **3** remained within the high-temperature-limiting regime. The relatively "open" coordination of the Zr centers in both amidozirconium derivatives thus reduces the steric interaction between the $\{MCp(CO)_2\}$ fragments and renders these compounds highly dynamic even at low temperatures. It also demonstrates that their stability is not simply the consequence of excessive steric shielding of the highly polar metal−metal bonds. Rather, as shown below, these compounds display a pronounced and characteristic reactive behavior.

Redistribution Reactions of 2 and 3 Involving the Metal Complex Fragments. Upon reaction of **2** and **3** with compound **1** in a molar ratio of 1:1, a quantitative complex fragment redistribution is observed that generates the dinuclear compounds $[CH_2(CH_2NSiMe_3)_2(Cl)Zr-FeCp(CO)_2]$ (**5**) and $[CH_2(CH_2NSiMe_3)_2(Cl)Zr-RuCp(CO)_2]$ (**6**), respectively (Scheme 2). A similar redistribution had been observed on reacting $[Cp_2Zr\{RuCp(CO)_2\}]$ with an equimolar amount of $[Cp_2ZrCl_2]$, giving $[Cp_2(Cl)Zr-RuCp(CO)_2]$.[24]

The almost identical positions of the ν(CO) bands in the infrared spectra of **2** and **5** as well as **3** and **6** indicate a similar metal−metal bonding situation in both types of complexes. The NMR spectra of both complexes are consistent with the rapid internal rotation around the metal−metal bonds over the temperature range down to 180 K, which is not surprising since the coordination sphere around Zr is even less crowded than that in the trinuclear complexes. The reduction in molecular symmetry upon the conversion of **2** and **3** to **5** and **6**, respectively, leads to a characteristic spectral pattern of the ^{1}H NMR resonances of the ligand backbone. The six methylene protons generate an AA′BB′CD spin system which results in the multiplet structure of compound **6** displayed in Figure 3. (See also Chart 3.) The ^{1}H nuclei of the N-bound methylene groups constitute the AA′BB′ part of the spectrum, the isochronous H^a and $H^{a'}$ protons (see Figure 3) being represented by a doublet of doublets of doublets at δ 3.40. The splitting pattern is due to the geminal coupling with H^b and $H^{b'}$ [$^2J(H^aH^b) = {}^2J(H^{a'}H^{b'}) = 13.0$ Hz] and vicinal coupling with H^c as well as H^d [$^3J(H^aH^c) = {}^3J(H^{a'}H^c) = 2.7$ Hz, $^3J(H^aH^d) = {}^3J(H^{a'}H^d) = 8.0$ Hz]. The assignment of H^c and H^d is based on the Karplus relationship for vicinal coupling in hydrocarbons.[51,52] The signal due to the H^b and $H^{b'}$ nuclei is observed at δ 3.21 and is also split into a doublet of doublets of doublets due to geminal and vicinal coupling with the H^c and H^d protons [$^3J(H^bH^c) = {}^3J(H^{b'}H^c) = 7.7$ Hz, $^3J(H^bH^d) = {}^3J(H^{b'}H^d) = 2.8$ Hz). The C

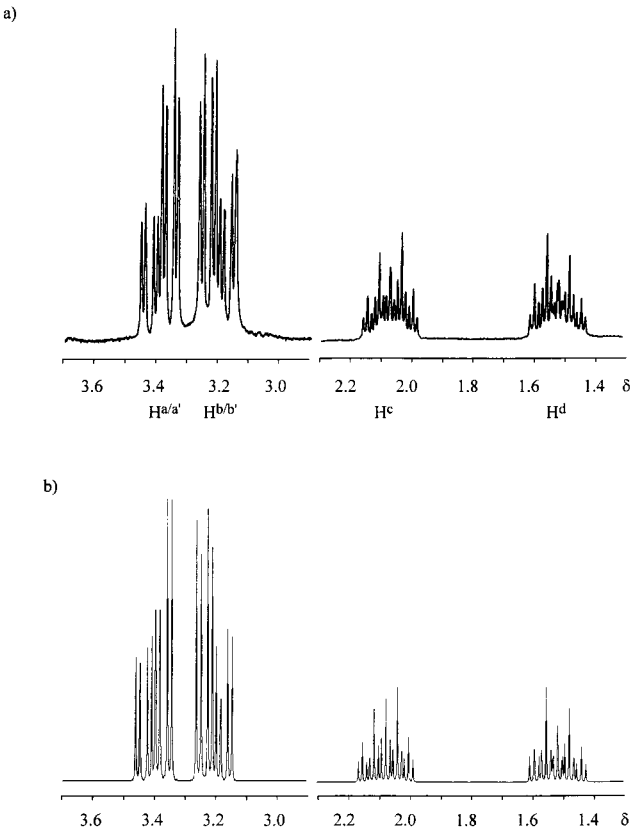

Figure 3. (a) ^{1}H NMR spectrum of **6** showing the AA′BB′CD multiplet structure of the $(CH_2)_3$ backbone of the chelating amido ligand. (b) Simulated ^{1}H NMR spectrum.

Chart 3

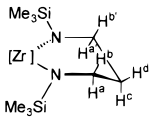

and D parts of the spectrum are represented by the two doublets of triplets of triplets at 1.52 (H^d) and 2.07 ppm (H^c). The geminal coupling constant $^2J(H^cH^d)$ was found to be 15.0 Hz. The interpretation of the complex coupling patterns observed for **5** and **6** was confirmed by simulation of the spectra using the parameters discussed above (Figure 4).[53]

It proved impossible to synthesize the corresponding Zr−Co heterodinuclear compound via the redistribution method which is most probably due to the thermal lability of the $ZrCo_2$ complex **4**. All attempts merely led to the isolation of the homonuclear cobalt dimer $[Co(CO)_3(PPh_3)]_2$, the product of a thermal redox degradation process. However, all three compounds **5**, **6**, and $[CH_2(CH_2NSiMe_3)_2(Cl)Zr-Co(CO)_3(PPh_3)]$ (**7**) cound be obtained, albeit in low yield, by reacting **1** with only 1 molar equiv of $K[MCp(CO)_2]$ (M = Fe, Ru) and $Na[Co(CO)_3(PPh_3)]$, respectively (Scheme 3).

The formation of a Zr−Co bond in compound **7** again may be inferred from the shift of the position of the carbonyl band (1963 cm^{-1}) in comparison with that of the carbonylmetalate anion (1839 cm^{-1}).[54] Furthermore, the ^{1}H and ^{13}C NMR spectra representing the amido complex fragment are essentially identical to those of **5** and **6**. Remarkably, the thermal stability of **7** in solution is significantly greater than that of the trinuclear species **4**.

(51) Karplus, M. *J. Chem. Phys.* **1959**, *30*, 11.
(52) Karplus, M. *J. Am. Chem. Soc.* **1963**, *85*, 2870.
(53) RACCOON: Program for the Simulation of NMR Spin Systems.
(54) Fischer, R. A.; Miehr, A.; Priermeier, T. *Chem. Ber.* **1995**, *128*, 831.

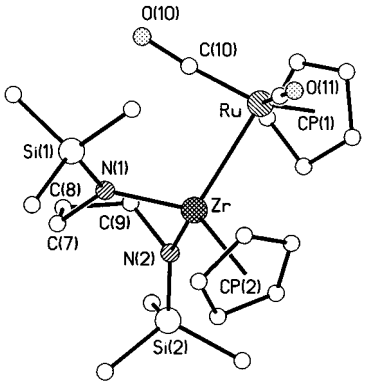

Figure 4. Molecular structure of $[CH_2(CH_2NSiMe_3)_2(Cp)Zr-RuCp(CO)_2]$ (**9**). The principal bond lengths and angles are listed in Table 2.

Scheme 3. Synthesis of **5**−**7** and Their conversion to **8**−**10**

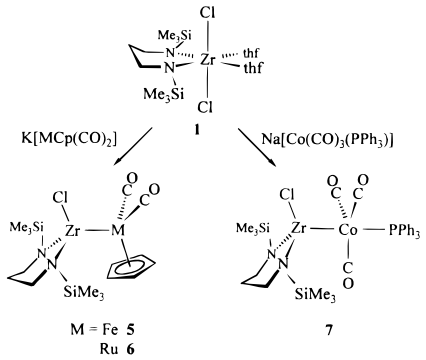

Attempts to generate a ZrFeRu heterotrimetallic compound by reacting **5** with $[RuCp(CO)_2]^-$ or **6** with $[FeCp(CO)_2]^-$ led to product mixtures in which the target compound could not be unambiguously identified. The facility of the Zr-bonded $\{MCp(CO)_2\}$ fragment to be displaced by a nucleophile, thus competing with Cl^-, is regarded as the underlying reason for this observation. That this is indeed a kinetic phenomenon and not a consequence of a redistribution equilibrium of the trinuclear complexes after their formation is inferred from the unsuccessful attempts to generate a trimetallic species through conproportionation of **2** and **3** even upon heating such mixtures in the absence or presence of additional chloride.

Reaction of compounds **5**−**7** with NaCp in toluene yields the previously reported heterodinuclear complexes $[CH_2(CH_2NSiMe_3)_2(Cp)Zr-MCp(CO)_2]$ (M = Fe (**8**), Ru (**9**)) and $[CH_2(CH_2NSiMe_3)_2(Cp)Zr-Co(CO)_3(PPh_3)]$ (**10**), respectively (Scheme 3).[41] This method provides an alternative to our original synthesis which was based on the salt metathesis of $[CH_2(CH_2NSiMe_3)_2Zr(Cp)Cl]$ with the carbonylmetalate salts and has provided crystals suitable for an X-ray structural study of **9** for the first time. The earlier structure analysis of **8** had revealed a Zr−Fe length of 2.745(1) Å, which, as mentioned above, is significantly longer than that in the $ZrFe_2$ compound **2**, but structural comparison with the unstable $[Cp_2Zr\{FeCp(CO)_2\}_2]$ or any related Cp_2Zr-Fe complex was not possible due to the absence of crystallographic data for these systems. In contrast, the structure analysis of the ZrRu compound (**9**) allows a direct comparison of it, the dinuclear compound of the bidentate amido ligand, and the corresponding trinuclear $ZrRu_2$ compound (**3**) with Casey's dinuclear,[24] Cp_2ZrRu, and trinuclear,[49] Cp_2ZrRu_2, compounds. Not unexpectedly, crystals of **9** were isomorphous with those of the previously investigated complex **8**, and the molecular structure displayed in Figure 4 is essentially identical to that of **8**.

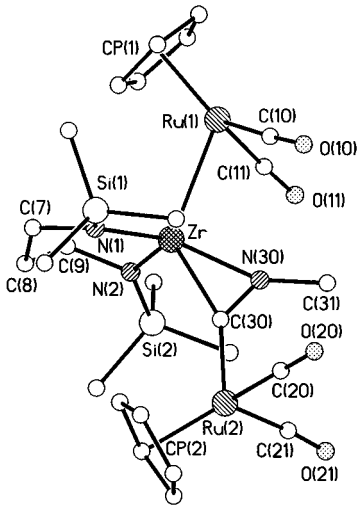

Figure 5. Molecular structure of the isonitrile monoinsertion product formed by **3**, the trinuclear compound $[CH_2(CH_2NSiMe_3)Zr\{\eta^2\text{-}C(=NMe)RuCp(CO)_2\}\{RuCp(CO)_2\}]$ (**16a**). Principal bond lengths and angles associated with the carbonyl, cyclopentadienyl, and bidentate ligands are listed in Table 2, and other selected parameters are as follows: Zr−N(30) 2.185(3), Zr−C(30) 2.237(4), Ru(2)−C(30) 2.040(4), N(3)−C(30) 1.278(5) Å; N(30)−Zr−C(3) 33.6(1), C(30)−Ru(2)−C(20) 88.9(2), C(30)−Ru(2)−C(21) 93.2(2), C(30)−Ru(2)−Cp(2) 118.2(3), Zr−C(30)−Ru(2) 153.6(2), Zr−N(30)−C(31) 155.1(3)°.

The structure of $[CH_2(CH_2NSiMe_3)_2(Cp)Zr-RuCp(CO)_2]$, **9**, which is isostructural with the iron analogue **8**, is shown in Figure 4. As observed in **8**, the halves of the molecule adopt a gauche conformation, the Cp ring of the ruthenium fragment occupying a staggered arrangement with respect to the $Me_3Si-N(2)$ unit and the Cp ligand at the zirconium center. Although the CO ligands are clearly bending toward the Zr atom [mean Zr−Ru−C(CO) 85.9(4)°], the Zr···C(CO) distances of 2.89(1) and 3.70(1) Å for C(10) and C(11), respectively, preclude any semibridging interaction. The Zr−Ru distance of 2.828(1) Å is considerably shorter than that of 2.910(1) Å in the dinuclear compound $[Cp_2(O^tBu)Zr-RuCp(CO)_2]$, but it is much longer than the two Zr−Ru bonds in **3**, the corresponding trinuclear compound of the bidentate amido ligand: Zr−Ru(1) 2.7372(7) and Zr−Ru(2) 2.7452 (7) Å (vide supra). The latter observation is the reverse of that in Casey's Cp_2Zr compounds, where the trinuclear compound has significantly *longer* Zr−Ru bonds [2.938(1) and 2.948(1) Å] than the dinuclear compound has [2.910(1) Å]; the lengthening of the Cp_2Zr-Ru bond in the trinuclear complex may be attributed to steric factors arising from the bulk of the four inflexible Cp ligands present (vide supra).

As in the case of **2** and **3**, in complex **9** unfavorable contact between the bulky trimethylsilyl groups and adjacent atoms are minimized by the flexibility of the trimethylsilyl-derivatized ligand, allowing the adoption of very large Zr−N−Si angles. The angles at N(1) and N(2) are 134.5(6) and 147.7(6)°, the latter extremely large angle being the result of the proximity of the bulky Cp(1) group; the gauche conformation of the two Cp rings means that Cp(2) is well away from both $SiMe_3$ substituents, allowing the relatively smaller angle at N(1). The geometry around each nitrogen donor is essentially planar [mean sum of angles at nitrogen 359(2)°].

Insertion of Isocyanides into the Zr−Fe and Zr−Ru Bonds. We previously interpreted the highly polar metal−metal bonds in the Zr−Fe and Zr−Ru heterodinuclear complexes as "masking" a pair of complex fragments acting as metal electrophiles and nucleophiles.[20] This reactive pattern is apparent

Scheme 4. Insertion of Methyl Isonitrile into the Metal−Metal Bonds of **5** and **6** as Well as **8** and **9** To Give **11**−**14**

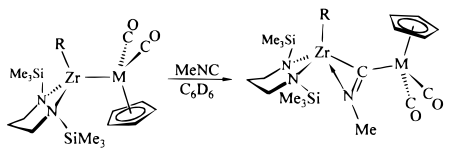

M	R	
Fe	Cl	**5**
Ru	Cl	**6**
Fe	Cp	**8**
Ru	Cp	**9**

M	R	
Fe	Cl	**11**
Ru	Cl	**12**
Fe	Cp	**13**
Ru	Cp	**14**

Scheme 5. Insertion of Isonitriles into One of the Zr−M Bonds in **2** and **3**

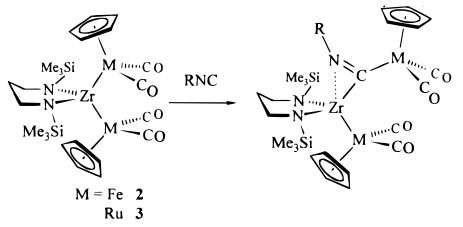

M	R	
Fe	Me	**15a**
	nBu	**15b**
	Cy	**15c**
	pTol	**15d**
Ru	Me	**16a**
	nBu	**16b**
	Cy	**16c**
	pTol	**16d**

in reactions with polar unsaturated organic substrates,[55] in particular, isonitriles which insert into the metal−metal bonds to give late transition metallaiminoacyl units coordinated in a side-on fashion to the zirconium centers. This reaction may also be understood as a metal analogue of the well-known α-addition to isonitriles.[56] Similar to other prevously studied heterobimetallic complexes, compounds **5** and **6** as well as **8** and **9** react immediately with methyl isonitrile to give the insertion products **11**−**14** (Scheme 4).

In view of this apparently general behavior of all Zr−Fe and Zr−Ru compounds previously studied by us, it was of particular interest to investigate the reactivity of the trinuclear complexes **2** and **3** toward isonitriles and especially to assess how the transformation at one Zr−M bond would affect the other. Compounds **2** and **3** react with 1 molar equiv of methyl, *n*-butyl, cyclohexyl, and *p*-tolyl isocyanide to yield the monoinsertion products **15a**−**d** and **16a**−**d**, repectively (Scheme 5). All monoinsertion products proved to be inert to a second equivalent or even a large excess of isonitrile, as was found by monitoring the reactions by ^{1}H NMR spectrocopy and reisolation of the starting materials.

The infrared spectra of **15a**−**d** and **16a**−**d** display a significant shift of ν(CO) bands in comparison to those of the starting materials: those of the C-bonded {MCp(CO)$_2$} fragments are shifted to higher wavenumbers while the Zr-bound {MCp(CO)$_2$} unit is shifted to significantly lower wavenumbers. The latter is particularly interesting since it indicates that insertion into one Zr−M bond indeed influences the second Zr−M bond. The charge redistribution between the directly metal−metal bonded donor and acceptor complex fragments in **15a**−**d** and **16a**−**d** appears to be significantly reduced and thus the residual electron density at the {MCp(CO)$_2$} fragment greater, as reflected in the IR data.

To obtain detailed information of the structural consequences of the isonitrile insertion, a single-crystal X-ray structure analysis of **16a** was carried out. The molecular structure is depicted in Figure 5, and the principal bond lengths and angles are listed in Table 2.

Similar to the cases of **2** and **3**, the central zirconium atom in **16a** adopts a distorted tetrahedral coordination geometry with the η^2-metallaiminoacyl ligand occupying one coordination site. The chelate ring adopts the conformation shown in Figure 5b, which differs from that of C_2 symmetry in **1** (and from the major component of the disorder in **2** and **3**), resulting in the SiMe$_3$ groups lying on the same side of the ring. The "flattened chair" conformation resembles that in the minor component of **2** and **3** (Figure 2b). Reduced steric strain at zirconium in **16a** is reflected in the smaller distortion of the Zr−N−Si angles, which are 126.5(2) and 134.7(2)° at N(1) and N(2), respectively, compared to a range of 132.5(6)−147.7(6)° in the other four structures.

The most remarkable feature is the increased length of the remaining Zr−Ru bond [d{Zr−Ru(2)} = 2.8639(6) Å] in **16a** compared to the mean Zr−Ru length of 2.7412(7) Å in the starting material **3**.

With the discussion related to the nature of the polar metal−metal bonds in mind, the reduction of the π-donor−acceptor interaction between the two metal centers resulting from the increased intermetallic distance may be responsible for the higher residual electron density at Ru(1), as manifested in the position of the ν(CO) bands in the IR spectrum. An increase of the metal−metal bond length should imply an enhanced reactivity toward a second equivalent of substrate, a notion which apparently contradicts the observed reactive behavior. In this context, we wish to re-emphasize that all isonitriles we employed give monoinsertion products. Isonitriles are very soft donor ligands, while the Zr atom is a very hard Lewis acid. We assume that, after the first insertion into a metal−metal bond and the concomitant reduction of the Lewis acidity of the zirconium (as a consequence of the increased coordination number and thus electron count), the initial acid−base interaction with the isonitrile, which we propose to be the first step in the insertion reaction, is not sufficiently strong anymore to effect the cleavage of the metal−metal bond and thus the α-addition of the metal electrophile and nucleophile to the substrate. On the other hand, as will be discussed below, other polar substrates such as sulfoxides will undergo far stronger Lewis acid−base interactions with the Zr center by virtue of both the greater polarity of their functional group and the HSAB principle and therefore react rapidly with both metal−metal bonds.

Cooperative Reactivity of Both Metal−Metal Bonds in 2−4 toward Sulfoxides. In view of the unexpected reaction of only one of the two metal−metal bonds in **2** and **3** with isocyanides, we were interested to find out whether this situation obtained in a type of reaction which is thermodynamically very strongly favored. Such a conversion is the deoxygenation of sulfoxides by early−late heterodinuclear complexes in which an oxygen atom transfer from the sulfoxide to a carbonyl ligand takes place to generate a linking CO_2 unit between the two metal centers.[57,58] (See Chart 4.) The reaction product of one of these transformations was unambiguously characterized by X-ray crystallography.[57,58] A remarkable aspect of this conversion is the extremely mild conditions under which the atom transfer takes place.[59−62] The reaction occurs essentially instantaneously even below − 40 °C.

(55) Memmler, H.; Kauper, U.; Gade, L. H.; Scowen, I. J.; McPartlin, M. *Chem. Commun.* **1996**, 1751.
(56) Saegusa, T.; Ito, Y. In *Organic Chemistry*; Ugi, I., Ed.; Academic Press: New York, 1971; Vol. 20.
(57) Fabre, S.; Findeis, B.; Trösch, D. J. M.; Gade, L. H.; Scowen, I. J.; McPartlin, M. *Chem. Commun.* **1999**, 577.
(58) Gade, L. H.; Schubart, M.; Findeis, B.; Fabre, S.; Bezougli, I.; Lutz, M.; Scowen, I. J.; McPartlin, M. *Inorg. Chem.* **1999**, *38*, 5282.
(59) Alper, H.; Keung, E. C. H. *Tetrahedron Lett.* **1970**, 53.
(60) Davies, S. G. *J. Organomet. Chem.* **1979**, *179*, C5.
(61) Alper, H.; Wall, G. *J. Chem. Soc., Chem. Commun.* **1976**, 263.
(62) Kukushkin, V. Y.; Moiseev, A. I. *Zh. Obshch. Khim.* **1990**, *60*, 692.

Chart 4

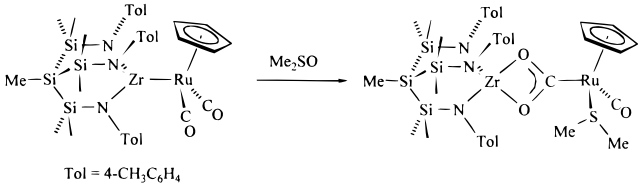

Scheme 6. Oxygen Transfer from Sulfoxides to Metal-Bound CO in the Conversion of **2** and **3** to **17a**−**c** and **18a**−**c**, Respectively

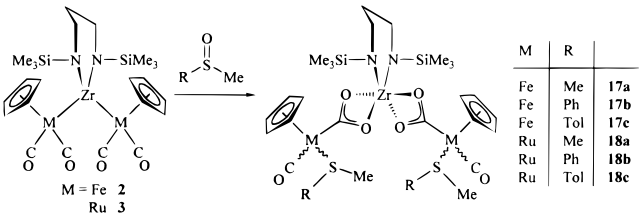

M	R	
Fe	Me	**17a**
Fe	Ph	**17b**
Fe	Tol	**17c**
Ru	Me	**18a**
Ru	Ph	**18b**
Ru	Tol	**18c**

Table 3. Positions of the ν(CO) and $\nu(\mu$-$CO_2)$ Bands in the Infrared Spectra of **17a**−**c** and **18a**−**c** and ^{13}C NMR Chemical Shifts of These Ligands

compd	ν(CO), cm^{-1}	$\nu(\mu$-$CO_2)$, cm^{-1}	$\delta(^{13}CO)^a$	$\delta(\mu$-$^{13}CO_2)^a$
17a	1949	1386, 1248	219.8	248.8, 249.0
17b	1941	1351, 1242	219.9	247.8, 247.9
17c	1942	n.o., 1247	220.0	248.3
18a	1940	1422, 1345	204.5, 204.6	231.4, 231.6
18b	1952	1375, 1290	204.5	230.4, 230.5
18c	1950	1348, 1258	204.5	230.8, 230.9

[a] The diastereotopic splitting of the ^{13}C NMR resonances is not always resolved.

Upon the reaction of **2** and **3** with 2 equiv of RS(O)Me (R = Me, Ph, Tol), an immediate conversion takes place to give the reaction products **17a**−**c** and **18a**−**c**, respectively (Scheme 6). The structural assignment is based on several very characteristic spectroscopic features which are summarized in Table 3. Since all compounds possess three centers of chirality (given the configurational instability of the donor atoms of the thioether ligands) of which the chiral center at zirconium is configurationally unstable on the NMR time scale, the signals of two sets of diastereomers (determined by the two chiral centers at ruthenium) are observed in the NMR spectra. In several cases, the signals of certain nuclear positions in the molecules coincide accidentally. In the IR spectra of all compounds, a single ν(CO) band is observed, indicating that one of the two carbonyl ligands present in the {MCp(CO)$_2$} units of the starting materials has been transformed in the reaction. The ^{13}C NMR resonances of the carbonyl ligands in **17a**−**c** appear at particularly low field as frequently observed for CpFe(CO)L units in which L is a soft donor ligand. The signals attributable to the bridging CO_2 unit are observed at δ 247−249 for **17a**−**c** and at δ 230.5−231.5 for **18a**−**c**, which is analogous to the case of previously characterized ZrM heterodinuclear compounds containing this structural element.[57,58] With the exception of those of **17c**, the resonances of the two diastereomers are resolved. The structural proposal put forward in Scheme 6 is additionally supported by the splitting of the ^{13}C NMR resonances assigned to the CH_2 groups adjacent to the N functions in the ligand backbone. For these methylene groups, three resonances are observed (for example, **18a**: δ 45.2, 45.4, 45.8) in an intensity ratio of 1:2:1. This is to be attributed to the presence of a racemate of the complex with an *R*,*R* or *S*,*S* configuration at the late transition metal center for which the two N-bound methylene carbon nuclei

Chart 5

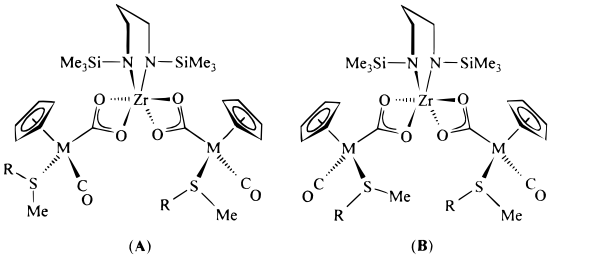

Scheme 7. Ejection of Insertion Isonitriles upon Conversion of **15a**−**d** and **16a**−**d** to **17a**−**c** and **18a**−**c**, Respectively

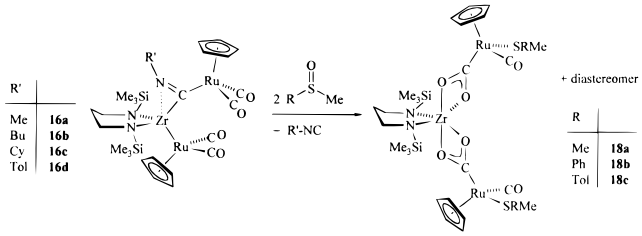

are chemically inequivalent (**A**), while the resonance with the double intensity is assigned to the *R*,*S*/*S*,*R* diastereomer ("meso"-diastereomer) (**B**). (See Chart 5.) On the basis of the detailed work of Gibson and co-workers on the infrared characteristics of the bridging CO_2 ligands,[63] we assign the bands listed in the second column of Table 3 to vibrations associated with this structural unit.

It proved impossible to isolate or even unambiguously detect reaction products of **2** and **3** with sulfoxides, in which only one of the two metal−metal bonds is broken while the other one remains intact as is the case in compounds **15a**−**d** and **16a**−**d**. On reaction of the heterotrinuclear complexes with only 1 molar equiv of sulfoxide, 50% of the starting materials are converted to compounds **17a**−**c** and **18a**−**c** while 50% remain unreacted. The oxygen transfer and cleavage of the metal−metal bonds in the trinuclear systems thus occur cooperatively; in other words, the reaction at one metal−metal bond enhances the reactivity of the other. The considerable thermodynamic driving force of this conversion (due to the formation of stable C−O and Zr−O bonds) is evident in the reaction of the isonitrile monoinsertion products **16a**−**d** with sulfoxides. In all cases, an immediate conversion to **18a**−**c** took place, the inserted isonitrile of the starting material being ejected from the metal−metal bond (Scheme 7).

Conclusions

The chemistry of early−late heterobimetallic complexes containing unsupported metal−metal bonds in which the early transition metal center is stabilized by a polydentate amido ligand has been extended to *difunctional* early transition metal building blocks. This has enabled the synthesis of heterotrinuclear complexes which in the case of the zirconium derivatives proved to be sufficiently stable to allow not only a full structural characterization but also the study of their reactive behavior. The latter is dominated by the possibility of complex fragment redistributions in the reaction with the dichlorozirconium starting materials and insertions into the highly polar metal−metal bonds as shown in the reactions with isonitriles. A more complicated

(63) Gibson, D. H.; Mehta, J. M.; Sleadd, B. A.; Mashuta, M. S.; Richardson, J. F. *Organometallics* **1995**, *14*, 4886.

reaction sequence is observed in the conversions with sulfoxides, leading to oxygen transfer from the sulfur reagent to metal-bound CO. Both the isonitrile insertion and the sulfoxide deoxygenation are reactions in which the two chemically complementary metal complex fragments bound to each other in the dinuclear complexes react in a *cooperative* manner with substrates.

Acknowledgment. We thank the Deutsche Forschungsgemeinschaft, the European Union (TMR program, network MECATSYN), the Fonds der Chemischen Industrie, the DAAD, and the British Council (Grant ARC 313 to L.H.G and M.M.) for financial support and Degussa AG as well as Wacker Chemie AG for generous gifts of basic chemicals.

Supporting Information Available: X-ray crystallographic files, in CIF format, for the structures of **1**, **2**, **3**, **9**, and **16a**. This material is available free of charge via the Internet at http://pubs.acs.org.

IC990350Q